NUCLEAR ENGINEERING

MASSACHUSETTS INSTITUTE
OF TECHNOLOGY

IMPACT OF THERMAL CONSTRAINTS ON THE OPTIMAL DESIGN OF HIGH-LEVEL WASTE REPOSITORIES IN GEOLOGIC MEDIA

Topical Report

C. Malbrain and R. K. Lester

August 1982

Department of Nuclear Engineering
Massachusetts Institute of Technology
Cambridge, Mass. 02139

MIT-NE-255

IMPACT OF THERMAL CONSTRAINTS ON THE OPTIMAL DESIGN OF HIGH-LEVEL WASTE REPOSITORIES IN GEOLOGIC MEDIA

Topical Report

C. Malbrain and R. K. Lester

August 1982

Department of Nuclear Engineering
Massachusetts Institute of Technology
Cambridge, Mass. 02139

Prepared for

THE U.S. DEPARTMENT OF ENERGY
AGREEMENT NO. EX-76-A-01-2295
TASK ORDER NO. 68

Impact of Thermal Constraints on the Optimal Design of High-Level Waste Repositories in Geologic Media

Carl Malbrain
Graduate Student

Richard K. Lester
Associate Professor

Department of Nuclear Engineering
Massachusetts Institute of Technology
Cambridge, Mass. 02139

July 2, 1982

Impact of thermal constraints on the optimal design of high-level waste repositories in geologic media

Abstract

An approximate, semi-analytical heat conduction model for predicting the time-dependent temperature distribution in the region of a high-level waste repository has been developed. The model provides the basis for a systematic, inexpensive examination of the impact of several independent thermal design constraints on key repository design parameters and for determining the optimal set of design parameters which satisfy these constraints. Illustrative calculations have been carried out for conceptual repository designs for spent pressurized water reactor (PWR) fuel and reprocessed PWR high-level waste in salt and granite media.

TABLE OF CONTENTS

LIST OF TABLES

LIST OF FIGURES

Nomenclature

α	= waste age at emplacement	(yrs)
α_t	= thermal expansion coefficient	($^oC^{-1}$)
c	= specific heat	(J/kg^oC)
d_r	= room-to-room spacing	(m)
D	= thermal diffusivity	(m^2/yr)
H	= repository depth	(m)
k	= thermal conductivity	($W/m\ ^oC$)
L_c	= active canister length	(m)
L_r	= room length of discrete line heat source region	(m)
m	= $\alpha_t\ (1+\nu)/(1-\nu)$	($^oC^{-1}$)
M_c	= canister mass loading	(MTHM)
ν	= Poisson's ratio	(-)
P	= canister pitch	(m)
q"	= areal heat source strength	($m\ ^oC/yr$)
q'"	= volumetric heat source strength	($^oC/yr$)
Q_c	= canister source strength	($m^3\ ^oC/yr$)
ρ	= density	(kg/m^3)
r	= radial distance from central canister centerline	(m)
R_h	= canister hole radius	(m)
t	= time since waste emplacement	(yrs)
T	= temperature	(^oC)
T_o	= initial temperature at repository midplane	(^oC)
u_z	= vertical rock displacement	(m)
w"	= areal heat generation rate	(W/m^2)

w''' = volumetric heat generation rate (W/m^3)

W_c = specific waste decay heat characteristics (W/MTHM)

z = depth below the surface (m)

1. Introduction

A key consideration in the design of underground repositories for the disposal of high-level waste is the radiogenic heat emitted by the waste canisters. The repository containment potential is affected by the decay heat in several ways. The high temperatures within the waste package itself tend to promote chemical reactions and physical changes in the waste form and surrounding engineered barriers which may enhance the leachability of the radionuclides. Elevated temperatures may also induce changes in the physical and chemical properties of the host rock. Groundwater flow behaviour in the vicinity of the repository may be modified by thermal stress fracturing in the host rock and neighboring strata, by buoyancy effects, or by other thermal phenomena. In addition, while the repository remains open, emplacement, monitoring, and potentially retrieval operations will all be complicated by the temperature increase.

Thermal design limits can be identified for each of the preceding phenomena, and such limits will play a central role in the design of high-level waste repositories. Exact quantification of these limits must await the selection of specific repository sites and waste package designs. In the meantime, generic thermal design criteria for alternative geologic media and package concepts have provided the basis for conceptual design efforts [1]. These efforts typically have involved the application of detailed, three-dimensional computer models for predicting the time-dependent temperature distribution in the region of the repository, such as the finite difference code HEATING 5[2]. Such codes readily account for the temperature dependence of the rock properties and provide detailed and accurate temperature estimates. Significant amounts of computer time are required, however, and the codes are therefore less suitable for parametric analyses of key repository design criteria. An approximate semi-analytical model, the Finite-Length Line Source Superposition Model (FLLSSM) has also been developed [3]. Though this code provides substantial savings, the need to superimpose the thermal contributions of each of the tens of thousands of canisters in a full-scale repository means that it is still quite time-consuming and costly to run. Since current thermal design limits and repository design concepts are still quite preliminary and likely to undergo substantial refinement, approximate models permitting more rapid and inexpensive estimates of repository thermal behaviour are particularly useful.

One such approximate model is presented here. The model differs in several important respects from FLLSSM: the use of analytical approximations for the waste decay heat behaviour and the homogenization of most of the individual heat sources in the repository each provide significant savings in computer time; in addition, the current model generates estimates of the time-dependent temperature distribution within the waste package itself; finally, the model estimates the far-field thermomechanical response of the geologic environment surrounding the repository. The model permits a systematic approach to the selection of combinations of key repository design and operating parameters which satisfy the various thermal criteria. Using a representative set of generic values for these criteria, the model has been applied to conceptual repository designs for spent pressurized water reactor (PWR) fuel and reprocessed PWR high-level waste in salt and granite media.

A primary focus of these applications was to investigate the impact on repository design of variations in the 'age' of the waste at the time of emplacement. At present, it seems unlikely that either spent fuel or reprocessed high-level waste will be placed in a full-scale repository until at least two decades after its generation. Recent proposals to establish monitored retrievable storage facilities (MRS) would, if implemented, increase the age at emplacement still further, perhaps by several decades.

2. Repository design features

Approximate analytical correlations describing the decay heat behaviour of the spent fuel and reprocessed high-level waste are shown in Table 1. The physical properties assumed for the salt and granite media are summarized in Table 2.

The waste package design concepts adopted for the analysis are based on those developed for the Swedish Kärnbränslesäkerhet (KBS) study [4]. The KBS waste packages were specifically designed so as to be compatible with the granitic environment expected for a Swedish repository. For convenience it is assumed here that the same packages would also be used in salt repositories. In the case of spent fuel, the fuel elements are disassembled and the rods placed in a thick-walled copper canister. The void space between the rods is filled with lead stabilizer. The canister is surrounded by a 20cm-thick buffer layer of highly compacted bentonite. The reference spent fuel package is shown in Figure 1. The reprocessed high-level waste is vitrified and cast in a cylindrical chromium-nickel steel container. The waste canister is surrounded by a 10cm-thick layer of lead and a thin outer sheath of titanium. The region between the titanium sheath and the rock wall is backfilled with a mixture of quartz sand (85%) and bentonite (15%). The reference high-level waste package is shown in Figure 2. The thermal properties assumed for the waste package materials are summarized in Table 3.

The repository layout assumed for these calculations is shown in Figure 3. Parallel horizontal rooms 1000 meters in length

Table 1

Analytical decay heat approximations for PWR spent fuel and reprocessed high-level waste [5].

Time (years)	Spent fuel[a] (Watts/MTHM)	Reprocessed high-level waste[b] (Watts/MTHM)[c]
$1 \leq t < 30$	$W_c(t) = 550 \exp(0.223 + 0.117t)^{-1}$	$W_c(T,t) = 363 \exp(0.257 + 0.083t)^{-1} + \Delta W_c(T,t)$
$30 \leq t < 300$	$W_c(t) = 9410t^{-0.749}$	$W_c(T,t) = 415t^{-0.752}\left[1 + \frac{15.3}{1+(\frac{t}{95})^4}\right] + \Delta W_c(T,t)$
$300 \leq t < 10^5$	$W_c(t) = 9410t^{-0.749}$	$W_c(T,t) = 415t^{-0.752} + \Delta W_c(T,t)$
		$\Delta W_c(T,t) = 141.3\,[e^{-0.0016T} - e^{-0.0482T}]e^{-0.0016t}$

a. Where t is years after reactor discharge.

b. Where t is years after reprocessing; and $(T + \frac{160}{365})$ is years between reactor discharge and reprocessing.

c. Where the basis is the quantity of high-level waste resulting from the reprocessing of 1 MTHM of spent fuel.

Table 2
Rock Properties

Property	Symbol	Salt	Granite
Density (kg/m^3)	ρ	2160	2646
Thermal conductivity (W/m^oC)	k	6.1	2.86
Heat capacity (J/kg^oC)	c	840	920
Thermal diffusivity (m^2/yr)	D	106	37.1
Thermal expansion coefficient ($^oC^{-1}$)	α_t	4.0×10^{-5}	8.1×10^{-6}
Poisson's ratio	ν	0.4	0.18

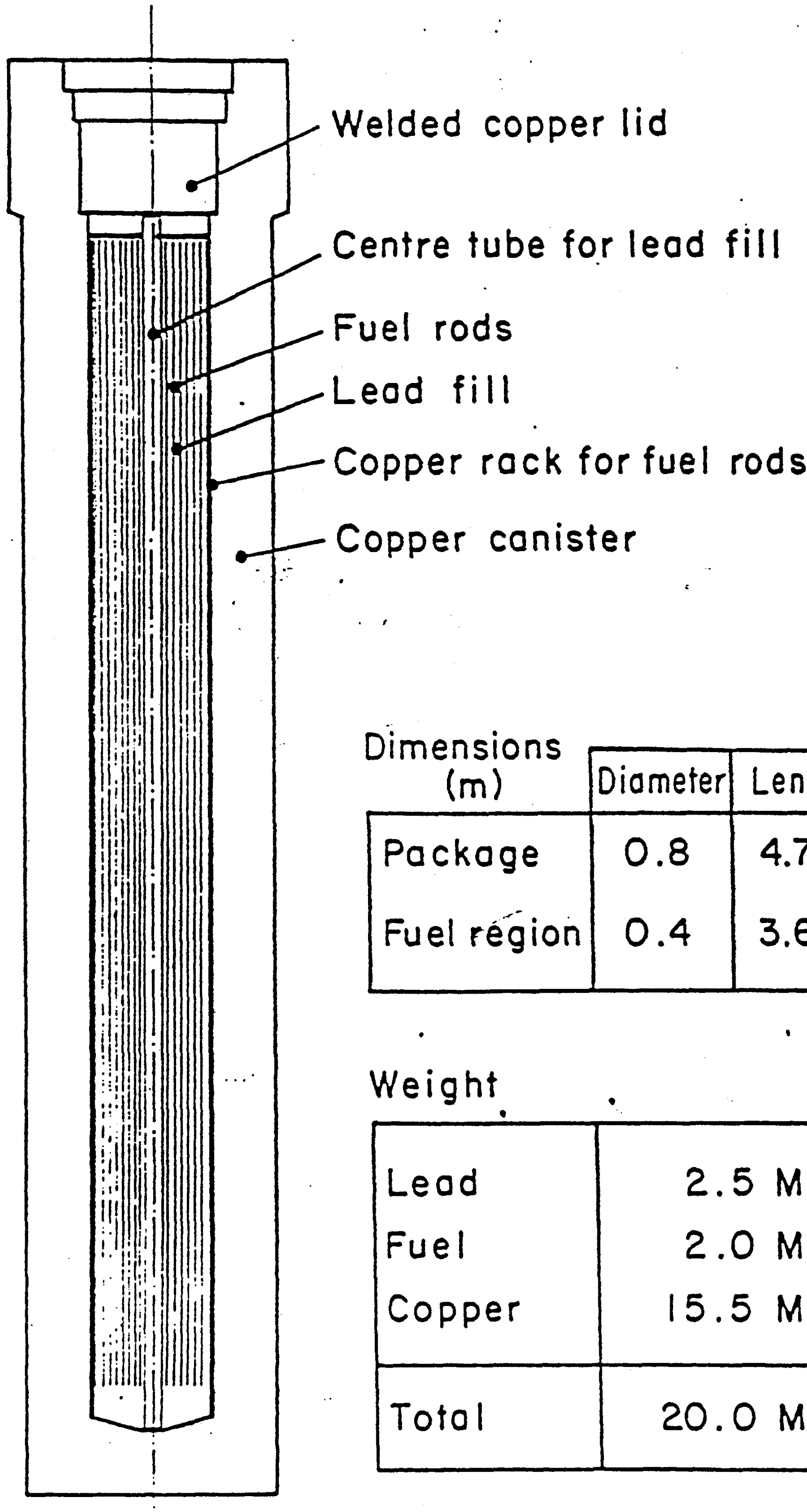

Dimensions (m)	Diameter	Length
Package	0.8	4.70
Fuel région	0.4	3.66

Weight

Lead	2.5 MT
Fuel	2.0 MT
Copper	15.5 MT
Total	20.0 MT

FIG. 1. [4]

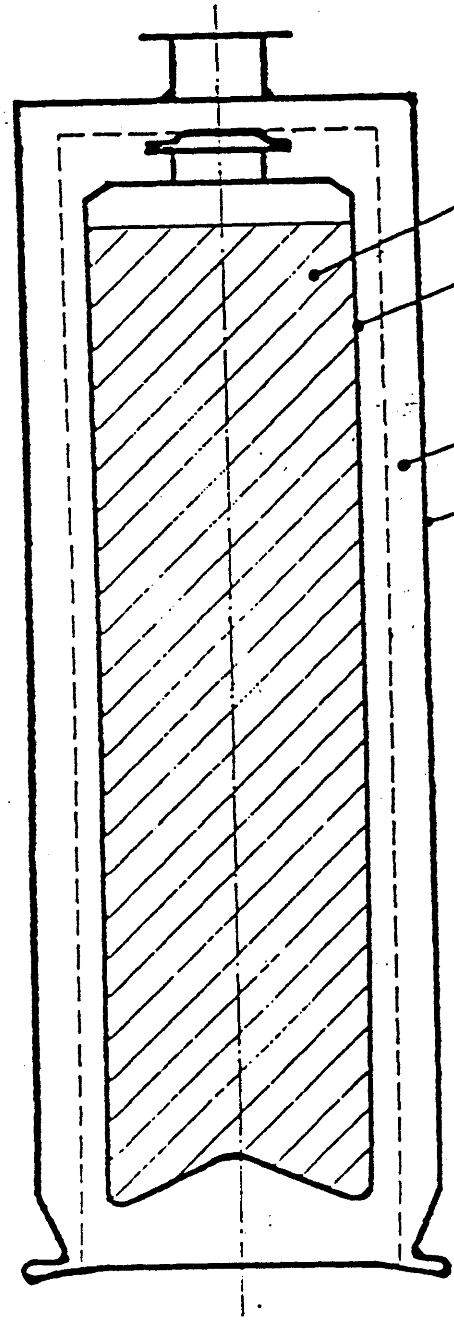

Dimensions (m)	Diameter	Length
Package	0.60	1.80
Waste	0.40	1.50

Weight

Lead	3.25 MT
Waste	0.45 MT
Total	3.70 MT

FIG. 2. [4]

Table 3
Waste package material properties

	ρ (kg/m^3)	k (W/m^oC)	c (J/kg^oC)	D (m^2/yr)
High-level waste[a]	3000	1.2	840	15.03
Lead[b]	11300	40	125	894
Copper	8940	400	400	3530
Bentonite[c]	2100	1.2	1000	18.03

a. The same properties were assumed for the spent fuel rods and vitrified high-level waste.

b. The impact of the thin titanium sheath on heat transfer in the waste package was neglected.

c. The same properties were assumed for the highly compacted bentonite and the quartz-bentonite mixture.

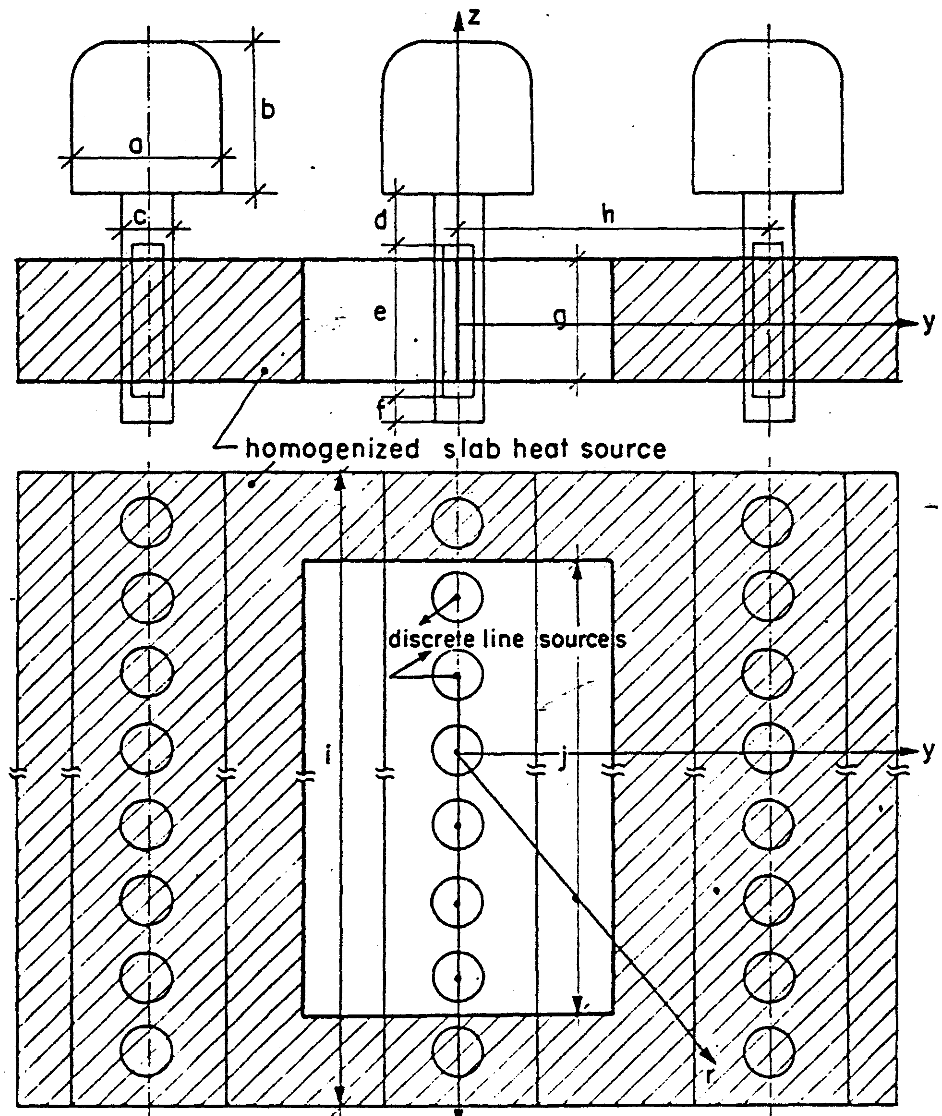

(m)	a	b	c	d	e	f	g	h	i	j
PWR-U/SF	5.50	6.70	1.00	2.50	4.70	0.50	3.66	25.0	1,000	70.0
PWR-U/HLW	5.50	6.10	1.20	1.50	1.80	0.50	1.50	25.0	1,000	70.0

FIG. 3.

separated by rock pillars 25 meters thick are excavated in the geologic formation at a depth of 600 meters. The waste canisters are placed in a single row of vertical holes drilled in the floor of each room. The rooms are connected to vertical shafts by horizontal access corridors at each end.

3. Thermal design limits

For the purposes of this analysis, four separate thermal criteria were adopted:

A. The maximum uplift at the surface over the repository due to thermal expansion should not exceed 1.5 meters. [6].

B. The maximum temperature in the host rock should not exceed 250°C in salt and 350°C in granite. [1].

C. The maximum temperature in the bentonite backfill layer should not exceed 100°C. [7].

D. The maximum centerline temperature should not exceed 500°C in the vitrified high-level waste canister [1] and 200°C in the spent fuel canister [7].

Both the selection of these criteria and the assignment of numerical values were to some extent arbitrary. Additional criteria have also been proposed in the literature. For example, limits on the temperature rise at the surface and in aquifers in the vicinity of the repository; limits on the volume of host rock exceeding threshhold temperatures; and limits on the temperature gradients established in the host rock [1]. Moreover, many of these criteria serve as proxies for underlying limits on rock mechanics, thermal hydraulic, or thermochemical phenomena which depend in complex ways on the repository environment and for which more detailed predictive calculations will be necessary once specific site characteristics are known. However, the simplified modelling approach adopted here is suitable for the present phase of conceptual design; moreover, additional thermal limits or changes in numerical values can readily be accommodated by the model.

In what follows, sets of values of the canister pitch, pillar thickness (i.e. room-to-room spacing), waste loading per canister, and waste age at emplacement which satisfy these thermal design limits are found.

4. Model Description

Three analytical or semi-analytical models were developed to predict the thermal behaviour in the far-field region, the near-field region, and within the waste package itself.

4.1 Far-field model

In the far-field region (i.e. at distances from the repository structure large compared with the spacing of individual canisters) heat transfer takes place almost entirely due to conduction. The basic equation of heat conduction for homogeneous, isotropic media is

$$\rho c \frac{\partial T}{\partial t} = \nabla . k \nabla T + w'''(\underline{r},t) \qquad (1)$$

where

T = rock temperature (^oC)

ρ = rock density (kg/m^3)

c = rock specific heat ($J/kg\ ^oC$)

k = rock thermal conductivity ($W/m\ ^oC$)

w''' = volumetric heat generation rate (W/m^3)

The geologic medium is represented as a semi-infinite, isotropic, homogeneous conducting material with a zero temperature boundary condition at the surface plane and an initial temperature everywhere zero. The physical properties of the medium are assumed to be temperature independent.

The repository itself is modelled as an infinite plane source at a depth corresponding to the midplane of the waste canisters, with a thermal strength equal to the average areal loading of the repository.

The temperature increase in the rock for the linearized, one-dimensional problem can be written:

$$T(z,t,\alpha) = \frac{1}{\sqrt{4\pi D}} \int_0^t q''(t+\alpha-\tau) \frac{1}{\sqrt{\tau}} \left\{ e^{\frac{-(z-H)^2}{4D\tau}} - e^{\frac{-(z+H)^2}{4D\tau}} \right\} d\tau \qquad (2)$$

where

z = depth below the surface (m)

H = repository depth (m)

t = time since waste emplacement (yrs)

α = waste age at emplacement (yrs)

D = thermal diffusivity (m^2/yr)

$= \frac{k}{\rho c} \cdot 3.156 \times 10^7$

$q''(t)$ = heat source strength for waste aged t years since generation (m^oC/yr)

$= \frac{w''}{\rho c} \cdot 3.156 \times 10^7$

w'' = areal heat generation rate (W/m^2)

If it is further assumed that the rock behaves as a thermo-elastic medium, the displacement due to thermal expansion is given by

$$u_z(z,t,\alpha) = \frac{m}{2} \int_0^t q''(t+\alpha-\tau) \left\{ \mathrm{erf}\left(\frac{z-H}{\sqrt{4D\tau}}\right) - \mathrm{erf}\left(\frac{z+H}{\sqrt{4D\tau}}\right) \right\} d\tau \qquad (3)$$

where

$$m = \alpha_t \left(\frac{1 + \nu}{1 - \nu} \right)$$

and

α_t = coefficient of thermal expansion ($^oC^{-1}$)

ν = Poisson's ratio

The uplift at the surface is given by:

$$u_z(0,t,\alpha) = -m\int_0^t q''(t+\alpha-\tau)\ \text{erf}\ \frac{H}{\sqrt{4D\tau}}\ d\tau \qquad (4)$$

For a given waste age at emplacement, α, it is easy to see from Equation (4) that the maximum surface uplift varies linearly with the initial thermal loading. It is thus straightforward to calculate for each value of α the initial thermal loading corresponding to a maximum allowable surface uplift limit of 1.5 meters. The corresponding mass loading (in kg/m^2) can then be obtained using the correlations in Table 1. The results are shown in Figure 4.

4.2 Near-field model

For the prediction of near-field temperatures in the host rock in the zone of maximum temperature (i.e. in the vicinity of the central canister in the central room), a semi-analytical three-dimensional model is constructed based on the following assumptions:

(i) The host rock is represented as an infinite, homogeneous, isotropic conducting medium with zero temperature at infinity.

(ii) The physical properties of the medium are temperature-independent.

(iii) The canisters are represented by finite-length line sources.

(iv) The volume actually occupied by the waste packages and the disposal rooms is assumed to have the same thermal properties as the host rock.

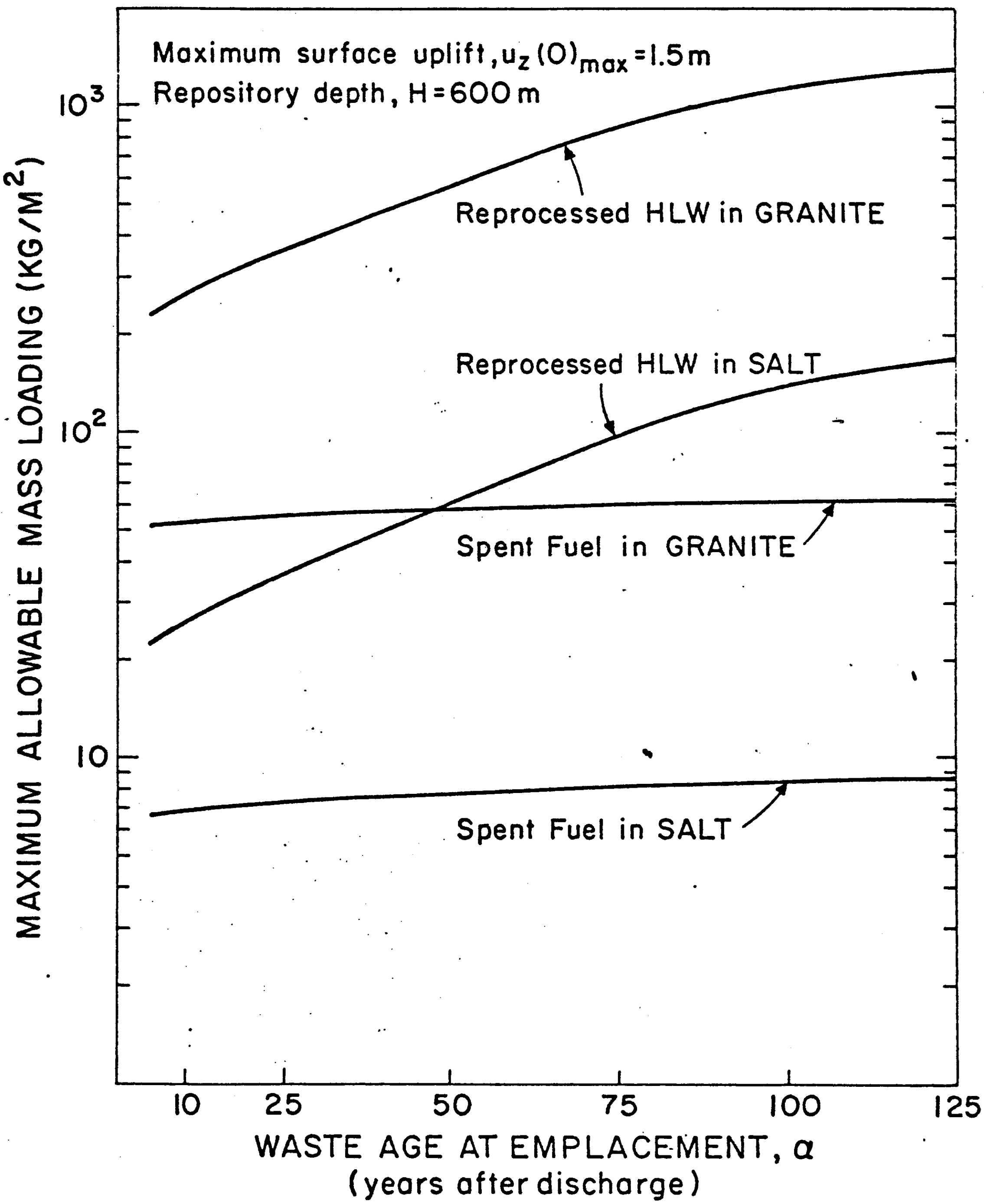
Maximum surface uplift, $u_z(0)_{max}$ = 1.5 m
Repository depth, H = 600 m
10^3
10^2
10
MAXIMUM ALLOWABLE MASS LOADING (KG/M^2)
Reprocessed HLW in GRANITE
Reprocessed HLW in SALT
Spent Fuel in GRANITE
Spent Fuel in SALT
10
25
50
75
100
125
WASTE AGE AT EMPLACEMENT, α
(years after discharge)

FIG. 4.

(v) Heat removal due to forced ventilation of the storage rooms and access corridors prior to backfilling is neglected.

(vi) The entire repository is instantaneously loaded with waste canisters of the same age.

(vii) The initial rock temperature at the repository midplane is 35°C.

To avoid the need to sum the thermal contributions of each of the tens of thousands of canisters stored in a full-scale repository, three further assumptions are made:

(viii) For all rooms except the central one, the row of discrete line sources is homogenized over a parallelepiped of length equal to the room length, width equal to the room-to-room spacing, and height equal to the active canister length.

(ix) To further simplify the integration, the rooms are assumed to be infinitely long.

(x) Within the central room, the canisters at distances greater than 35 meters from the center are homogenized into parallelepiped sources.

The near-field model geometrical assumptions are illustrated in Figure 3.

Solution of the heat conduction equation (1) for the peak host rock temperature location (i.e. at the rock-package interface for the centeral waste canister in the repository midplane) yields:

$$T(R_h,t,\alpha) = T_o + \frac{1}{4\pi DL_c}\int_0^t \frac{Q_c(t+\alpha-\tau)}{\tau} e^{-R_h^2/4D\tau} \operatorname{erf}\frac{L_c}{4\sqrt{D\tau}}\, d\tau +$$

$$+ \frac{1}{2\pi DL_c} \sum_{i=1}^{N} \int_0^t \frac{Q_c(t+\alpha-\tau)}{\tau} e^{-d_i^2/4D\tau} \operatorname{erf}\frac{L_c}{4\sqrt{D\tau}}\, d\tau + \qquad (5)$$

$$+ \frac{1}{d_r P L_c}\int_0^t Q_c(t+\alpha-\tau) \operatorname{erf}\frac{L_c}{4\sqrt{D\tau}}\, d\tau -$$

$$- \frac{1}{2d_r P\, L_c}\int_0^t Q_c(t+\alpha-\tau)\left\{\operatorname{erf}\frac{R_h+d_r/2}{\sqrt{4D\tau}} - \operatorname{erf}\frac{R_h-d_r/2}{\sqrt{4D\tau}}\right\} \operatorname{erf}\frac{L_r}{4\sqrt{D\tau}} \operatorname{erf}\frac{L_c}{4\sqrt{D\tau}}\, d\tau$$

where T_o is the initial temperature at the repository midplane, the second term predicts the temperature increment at the hole-wall due to the central waste canister, the third term the contribution of the adjacent discrete line sources in the central room, and the last two terms account for the contribution of the surrounding homogenized source. In Equation (5):

P = canister pitch (m)

$(2N + 1)$ = number of discrete line sources

L_r = $(2N + 1)P \geq 70$ (m)

L_c = active canister length (m)

R_h = hole radius (m)

d_r = room-to-room spacing (m)

d_i^2 = $R_h^2 + (iP)^2$

and

$$Q_c(t) = \frac{3.156 \times 10^7}{\rho c} M_c\, W_c\,(t) \quad (m^3\ {}^oC/yr)$$

where $W_c(t)$ = waste decay heat, from Table 1 (W/MTHM)

M_c = canister mass loading (MTHM)

Quantitative error estimates were obtained for most of the preceding assumptions. The error in the near-field temperature introduced by the infinite geologic medium assumption was found not to become significant until well after the maximum temperature in the mid-plane occurred. Also, for expected full-scale repository horizontal dimensions on the order of 1000 meters, the error in the maximum near-field temperature introduced by assuming an infinite room length was also found to be insignificant. The finite length line source approximations contained in assumptions (iii) and (iv) were found elsewhere to yield errors of less than 3% in the maximum rock wall temperature. [8]. Assumptions (vii) and (ix) regarding heat source homgenization were also found to result in a combined error of less than 3%.

More significant errors were introduced by neglecting the temperature dependence of the rock thermal conductivity. A three-dimensional near-field calculation with temperature-dependent thermal properties was not attempted here. However, when the temperature-dependent thermal conductivity of salt was incorporated into a one-dimensional calculation for a high-level waste repository, the maximum temperature was 17% higher than when an average value was assumed. Another potentially significant source of error, which leads to conservative design predictions, is the neglect of forced ventilation heat removal from the storage rooms prior to backfilling.

The effects of some of these assumptions are presented in more detail in Appendix I.

4.3 Waste package model

To predict the temperature distribution within the waste package, a simple one-dimensional, quasi-steady state model was adopted. The one-dimensional steady state heat conduction equation for the cylindrical coordinate system

$$\frac{D}{r}\frac{\partial}{\partial r}\left(r \frac{\partial T}{\partial r} \right) + q'''(\underline{r},t) = 0 \tag{6}$$

is solved for the waste package region at successive time steps, at each time imposing as the rock-package interface boundary condition the temperature predicted by Equation (5). As a result, the temperature at the canister outer surface is given by:

$$T(R_{co},t,\alpha) = T(R_h,t,\alpha) + \frac{W_c(t+\alpha)M_c}{2\pi k_b L_c} \ln \frac{R_h}{R_{oc}} \tag{7a}$$

at the canister inner surface:

$$T(R_{ci},t,\alpha) = T(R_{co},t,\alpha) + \frac{W_c(t+\alpha)M_c}{2\pi k_c L_c} \ln \frac{R_{oc}}{R_{ic}} \tag{7b}$$

and at the canister centerline:

$$T(o,t,\alpha) = T\ (R_{ci},t,\alpha) + \frac{W_c(t+\alpha)M_c}{4\pi k_w L_c} \tag{7c}$$

where k_b, k_c, k_w represent the conductivities of the backfill, canister and waste materials respectively. For the spent fuel package calculations, the fuel rod-lead stabilizer region was homogenized.

5. Results

5.1 Fixed canister loadings

The preceding models were applied to spent fuel and reprocessed high-level waste repositories in salt and granite. In all cases, a room-to-room spacing of 25 meters was assumed. The spent fuel canisters contained two PWR assemblies (0.9228 MTHM), and the high-level waste canisters contained the waste products from the reprocessing of 1 MTHM of spent fuel. In each case, the maximum temperatures in the rock, backfill, and waste matrix were computed as a function of the waste age at emplacement and the canister pitch. The calculated maximum temperatures in the backfill are illustrated in Figure 5(a)-(d).

5.2 Sensitivity of repository loadings to design parameters

The sensitivity of the maximum permissible repository mass loading to some of the repository design parameters, such as backfill material conductivity, room-to-room distance, and the number of canisters per hole, was investigated. The maximum allowable backfill temperature of 100°C was the only thermal design limit considered in these calculations. Details of the results of these calculations are presented in Appendix II.

5.2.1 Backfill conductivity

To account for possible reductions in thermal conductivity as a result of the elevated temperatures or because of fracturing of the backfill layer, the average backfill material conductivity was reduced by a factor of three, to 0.4 W/m°C. The effect on the repository mass loading is shown in Table 1 of Appendix II. The reduction in repository loading is significant for young waste ages

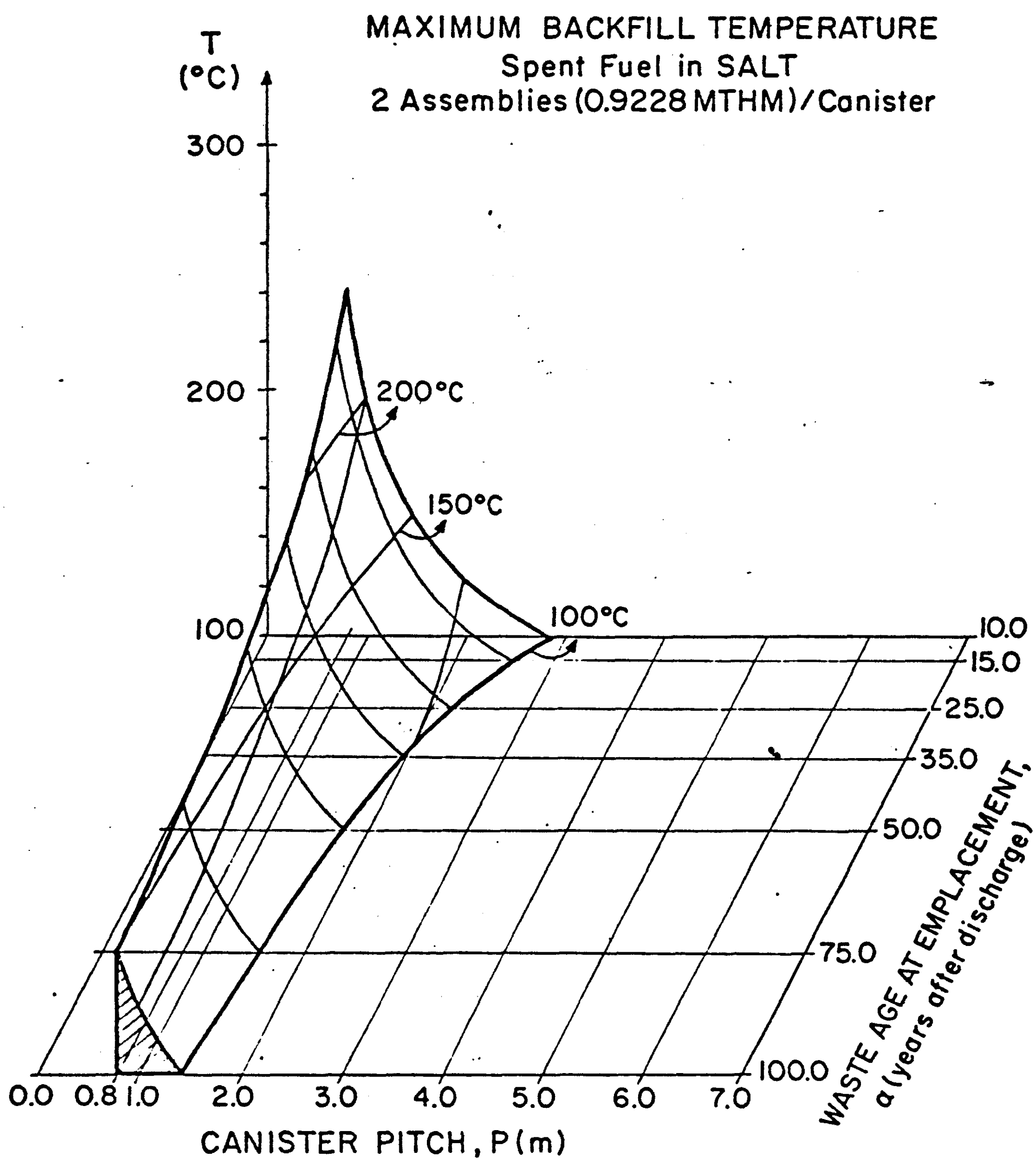
MAXIMUM BACKFILL TEMPERATURE
Spent Fuel in SALT
2 Assemblies (0.9228 MTHM)/Canister
T
(°C)
300
200
100
200°C
150°C
100°C
10.0
15.0
25.0
35.0
50.0
75.0
100.0
0.0
0.8
1.0
2.0
3.0
4.0
5.0
6.0
7.0
CANISTER PITCH, P(m)
WASTE AGE AT EMPLACEMENT,
α (years after discharge)

FIG. 5(a)

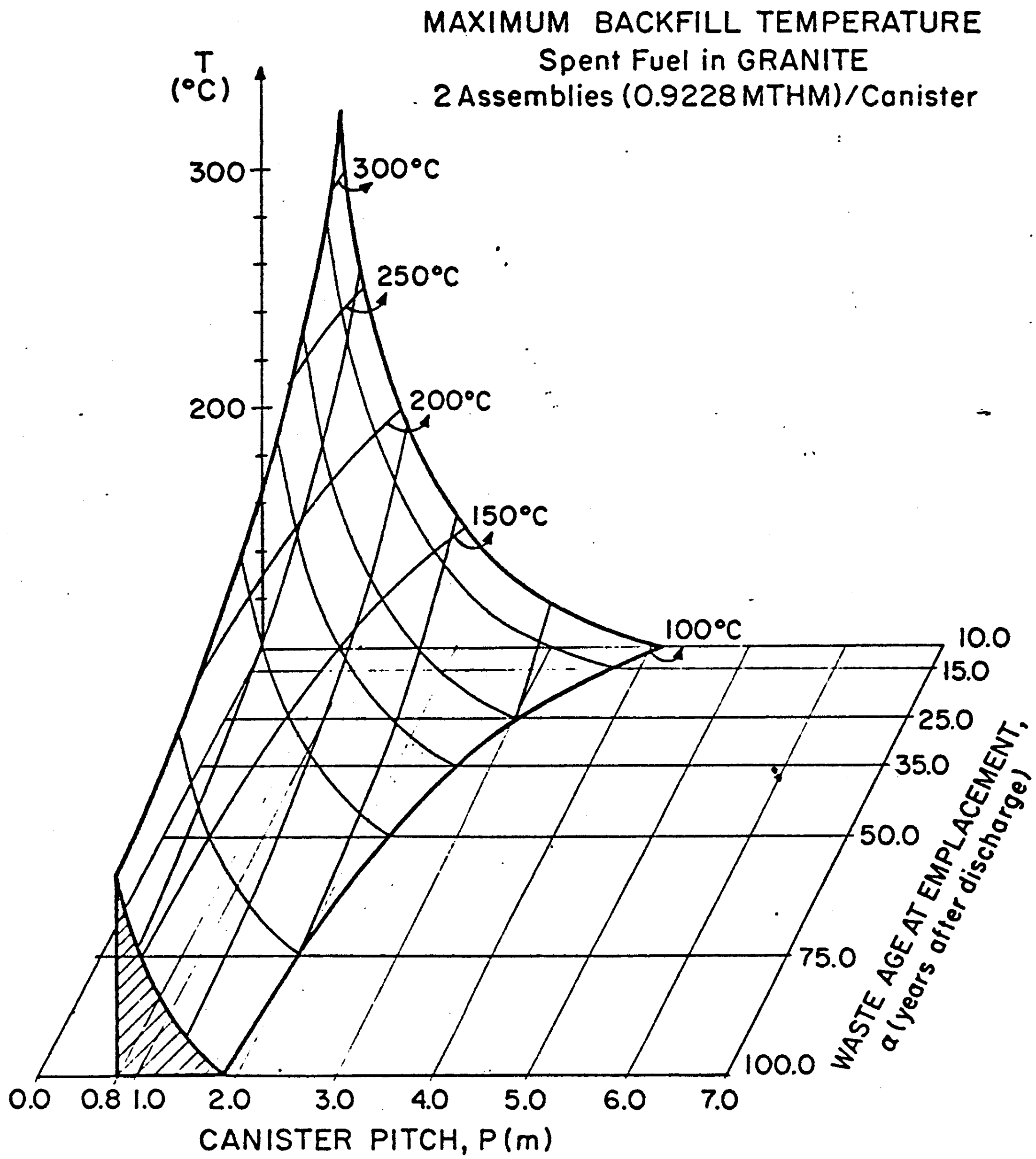
MAXIMUM BACKFILL TEMPERATURE
Spent Fuel in GRANITE
2 Assemblies (0.9228 MTHM)/Canister
T
(°C)
300
200
300°C
250°C
200°C
150°C
100°C
10.0
15.0
25.0
35.0
50.0
75.0
100.0
WASTE AGE AT EMPLACEMENT,
α (years after discharge)
0.0
0.8
1.0
2.0
3.0
4.0
5.0
6.0
7.0
CANISTER PITCH, P (m)

FIG. 5(b)

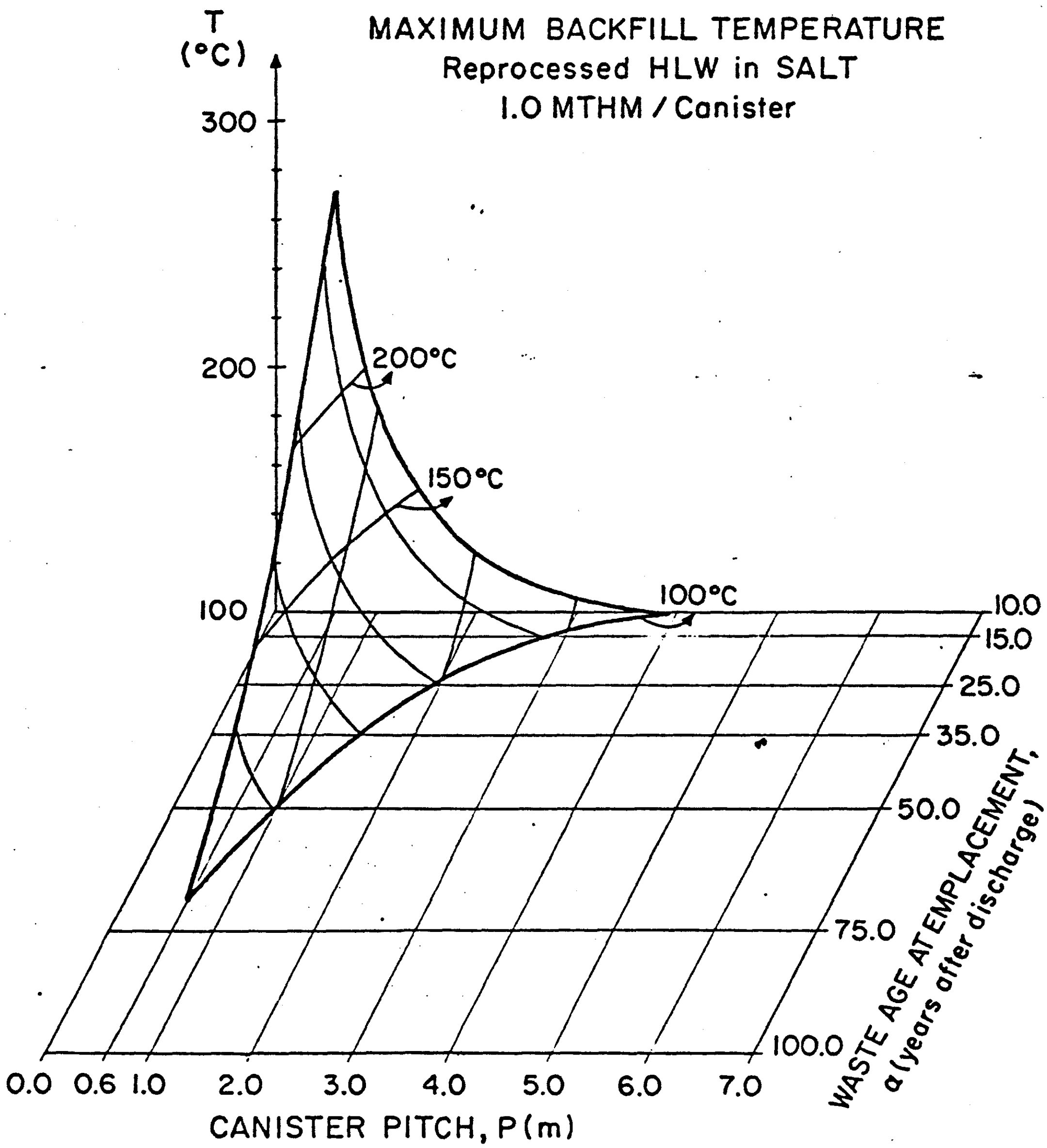
T
(°C)
MAXIMUM BACKFILL TEMPERATURE
Reprocessed HLW in SALT
1.0 MTHM / Canister
300
200
100
200°C
150°C
100°C
10.0
15.0
25.0
35.0
50.0
75.0
100.0
WASTE AGE AT EMPLACEMENT,
a (years after discharge)
0.0
0.6
1.0
2.0
3.0
4.0
5.0
6.0
7.0
CANISTER PITCH, P(m)

FIG. 5(c)

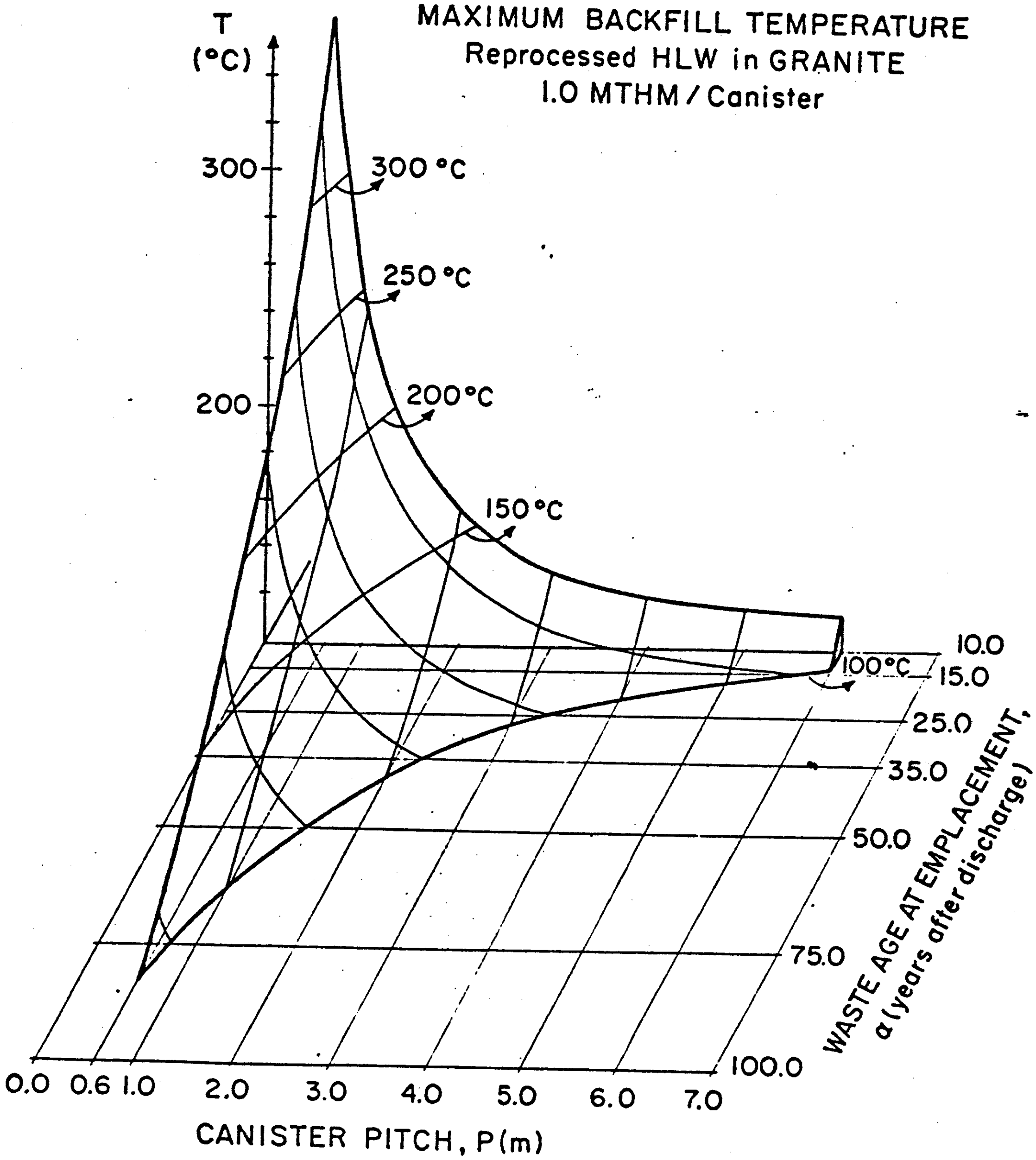
MAXIMUM BACKFILL TEMPERATURE
Reprocessed HLW in GRANITE
1.0 MTHM / Canister
T
(°C)
300
200
300 °C
250 °C
200°C
150 °C
100°C
10.0
15.0
25.0
35.0
50.0
75.0
100.0
WASTE AGE AT EMPLACEMENT,
α (years after discharge)
0.0
0.6
1.0
2.0
3.0
4.0
5.0
6.0
7.0
CANISTER PITCH, P(m)

FIG. 5(d)

at the time of emplacement. However, the effect of changing the backfill material conductivity declines as the age of the waste of emplacement of the wastes is increased.

5.2.2 Waiting time prior to hole backfilling.

In order not to violate the backfill temperature limit of 100°C, the backfilling of the holes with bentonite blocks once the canisters are emplaced could be postponed for a certain period of time. The required waiting times prior to backfilling after the emplacement of the reprocessed HLW canisters are shown in Figure 6 (a)-(b). In these calculations, heat removal due to forced ventillation of the storage rooms and access corridors was neglected. The effect of a 25.0 year waiting period prior to backfilling on the repository mass loading is shown in App. II, Table 2. Increased aging of the waste prior to emplacement will again reduce the effect of the prior-to-backfill waiting period. In the case of spent fuel, the case for delaying the initiation of backfilling is weaker. The maximum rock temperature occurs at much longer times after emplacement and declines much less rapidly thereafter because of the slower decay behavior of the spent fuel. This can be seen from the temperature histograms in Figure 7(a)-(b) compared to those for reprocessed HLW (Figure 7(c)-(d)).

5.2.3 Room-to-room distance

In the conceptual repository design, the room-to-room distance was arbitrarely taken to be equal to 25.0m in order to maintain the structural stability of the rooms and pillars. It is conceivable, however, that a higher extraction ratio will be possible without

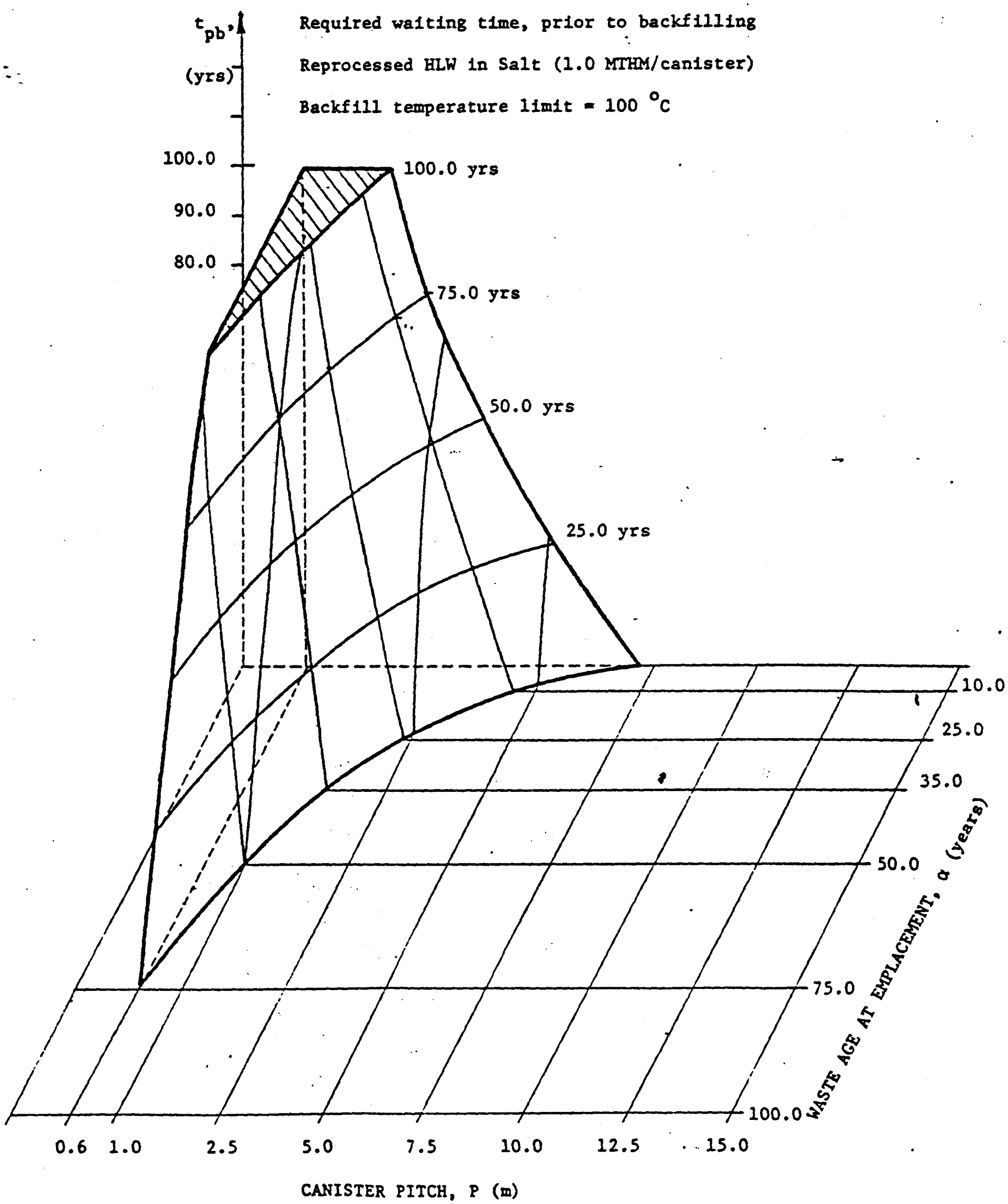

t_pb, (yrs)
Required waiting time, prior to backfilling
Reprocessed HLW in Salt (1.0 MTHM/canister)
Backfill temperature limit = 100 °C
100.0
90.0
80.0
100.0 yrs
75.0 yrs
50.0 yrs
25.0 yrs
10.0
25.0
35.0
50.0
75.0
100.0
WASTE AGE AT EMPLACEMENT, α (years)
0.6
1.0
2.5
5.0
7.5
10.0
12.5
15.0
CANISTER PITCH, P (m)

Figure 6(a)

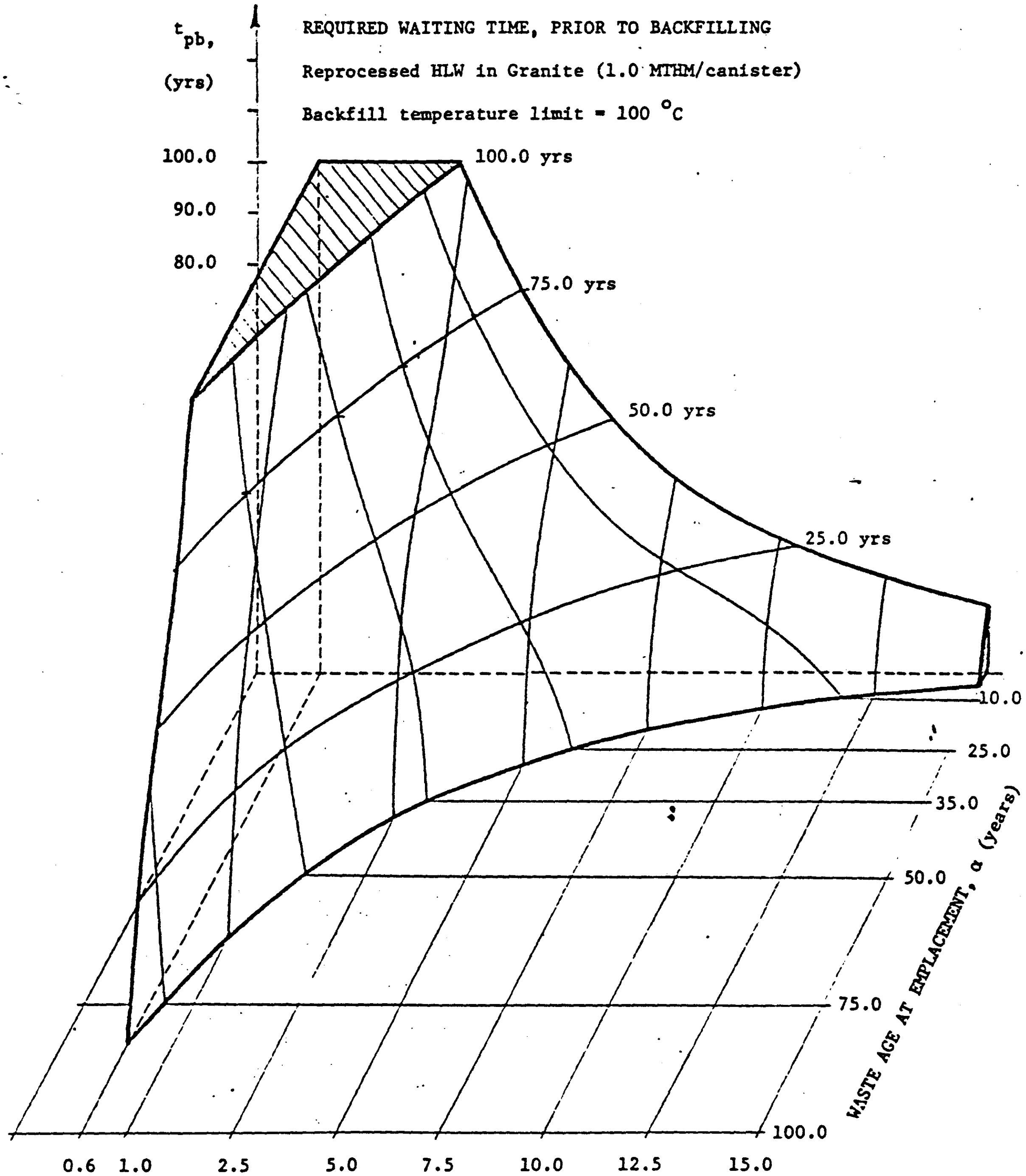
t_pb, (yrs)
REQUIRED WAITING TIME, PRIOR TO BACKFILLING
Reprocessed HLW in Granite (1.0 MTHM/canister)
Backfill temperature limit = 100 °C
100.0
90.0
80.0
100.0 yrs
75.0 yrs
50.0 yrs
25.0 yrs
10.0
25.0
35.0
50.0
75.0
100.0
WASTE AGE AT EMPLACEMENT, α (years)
0.6
1.0
2.5
5.0
7.5
10.0
12.5
15.0
CANISTER PITCH, P (m)

Figure 6(b)

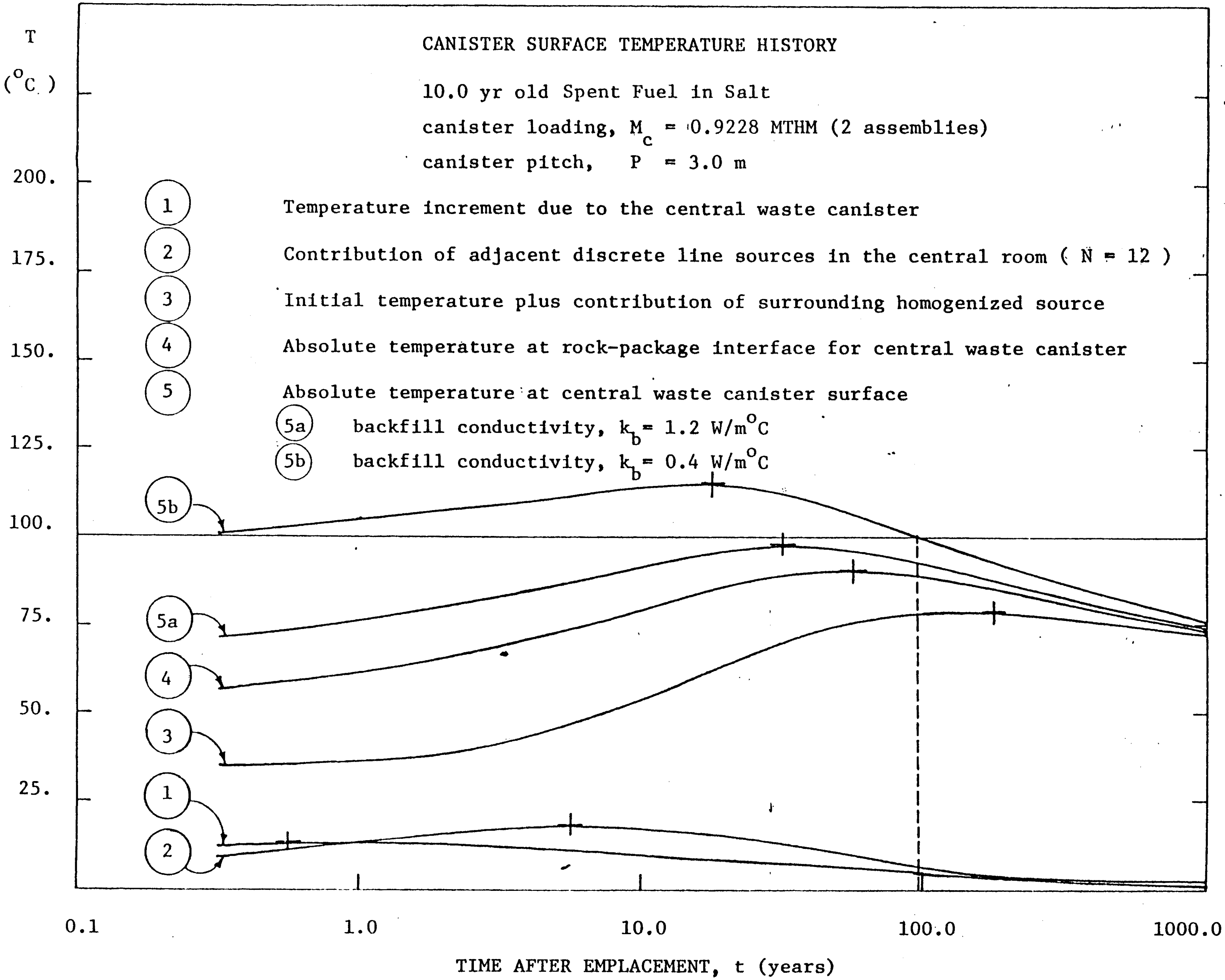
CANISTER SURFACE TEMPERATURE HISTORY
10.0 yr old Spent Fuel in Salt
canister loading, M_c = 0.9228 MTHM (2 assemblies)
canister pitch, P = 3.0 m
1 Temperature increment due to the central waste canister
2 Contribution of adjacent discrete line sources in the central room (N = 12)
3 Initial temperature plus contribution of surrounding homogenized source
4 Absolute temperature at rock-package interface for central waste canister
5 Absolute temperature at central waste canister surface
5a backfill conductivity, k_b = 1.2 W/m°C
5b backfill conductivity, k_b = 0.4 W/m°C
T (°C)
200.
175.
150.
125.
100.
75.
50.
25.
5b
5a
4
3
1
2
0.1
1.0
10.0
100.0
1000.0
TIME AFTER EMPLACEMENT, t (years)

Figure 7a

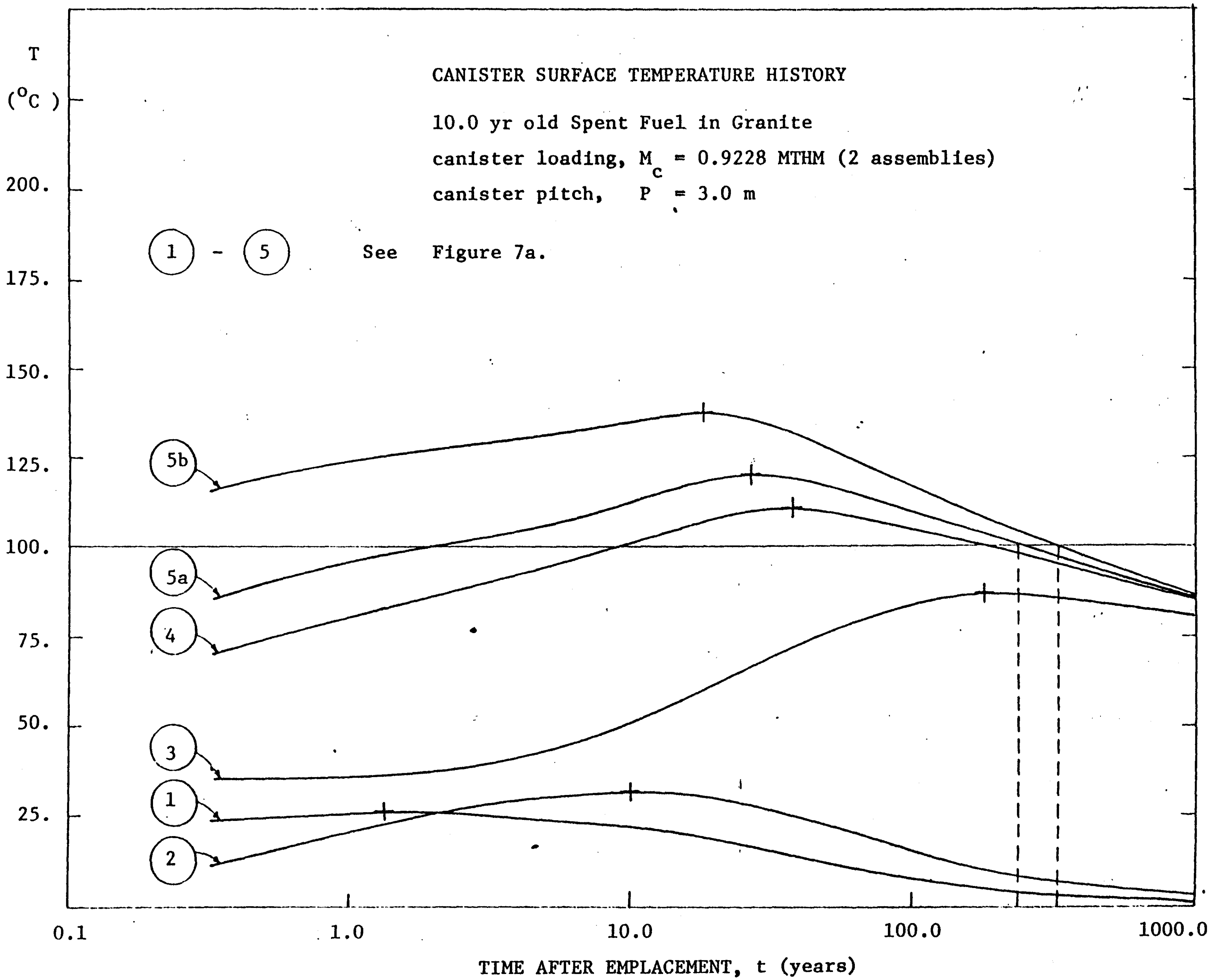
T
(°C)
200.
175.
150.
125.
100.
75.
50.
25.
CANISTER SURFACE TEMPERATURE HISTORY
10.0 yr old Spent Fuel in Granite
canister loading, Mc = 0.9228 MTHM (2 assemblies)
canister pitch, P = 3.0 m
1 - 5 See Figure 7a.
5b
5a
4
3
1
2
0.1
1.0
10.0
100.0
1000.0
TIME AFTER EMPLACEMENT, t (years)

Figure 7b

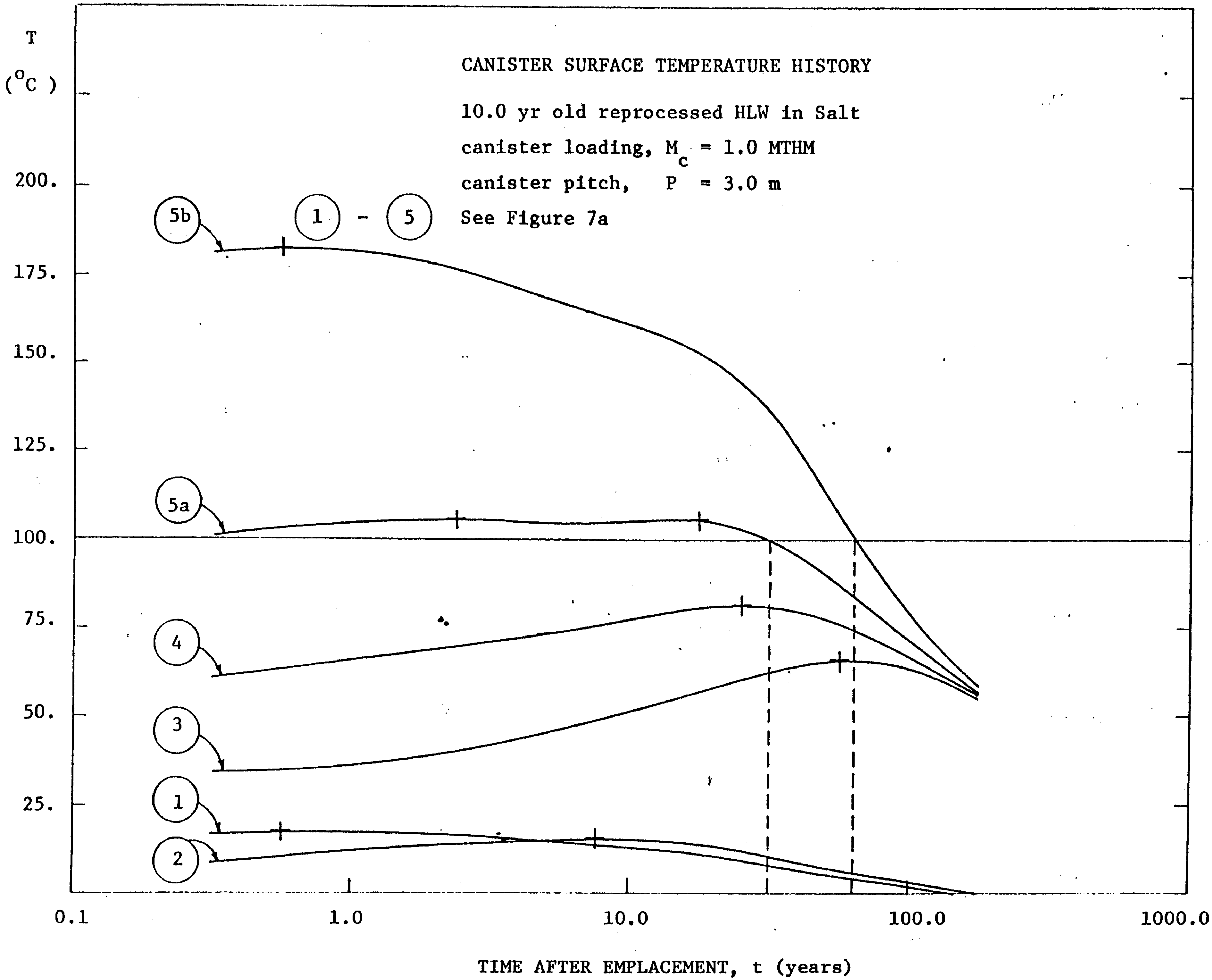

CANISTER SURFACE TEMPERATURE HISTORY
10.0 yr old reprocessed HLW in Salt
canister loading, M_c = 1.0 MTHM
canister pitch, P = 3.0 m
1 - 5 See Figure 7a
T (°C)
200.
175.
150.
125.
100.
75.
50.
25.
5b
5a
4
3
1
2
0.1
1.0
10.0
100.0
1000.0
TIME AFTER EMPLACEMENT, t (years)

Figure 7c

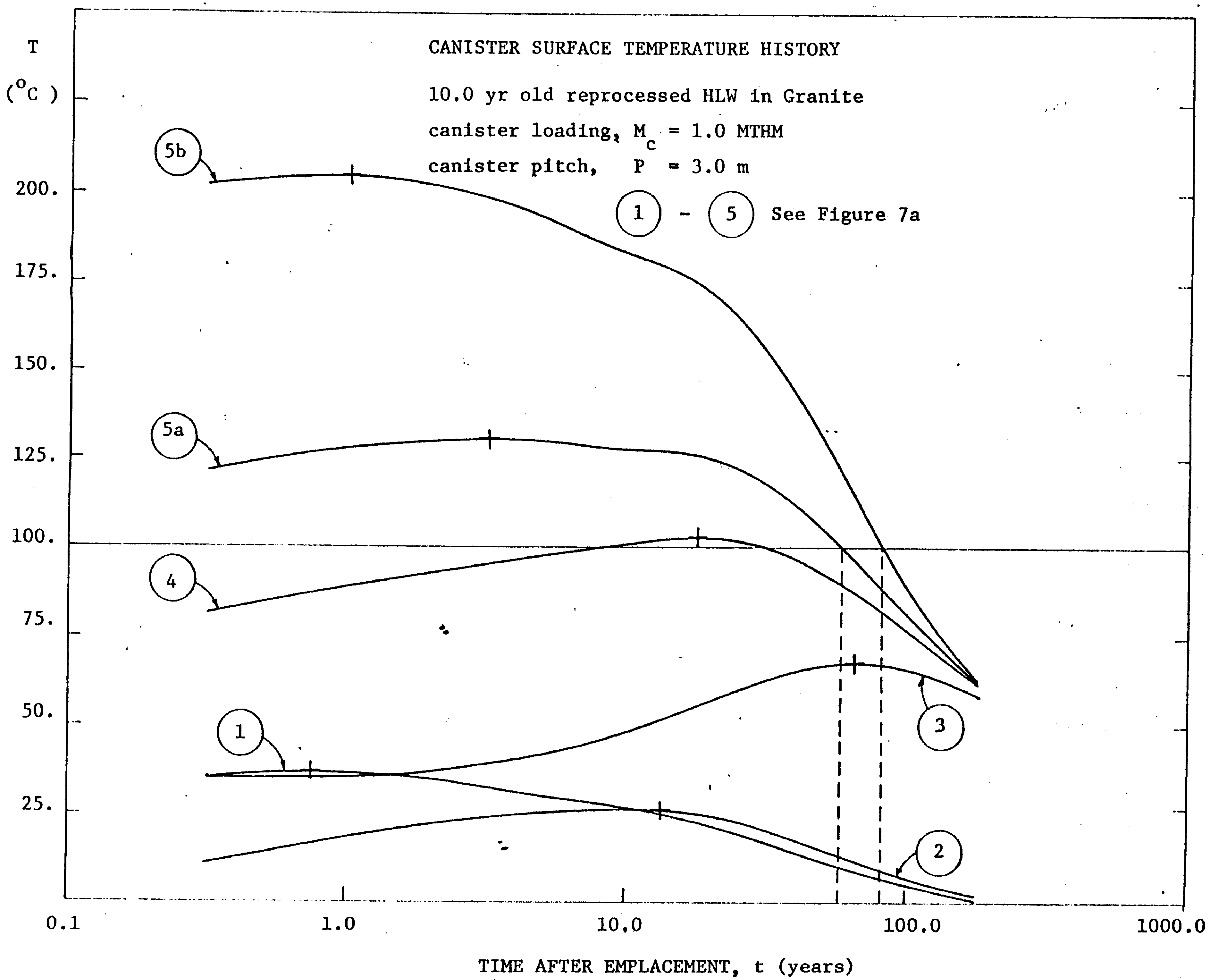
CANISTER SURFACE TEMPERATURE HISTORY
10.0 yr old reprocessed HLW in Granite
canister loading, M_c = 1.0 MTHM
canister pitch, P = 3.0 m
1 - 5 See Figure 7a
T
(°C)
200.
175.
150.
125.
100.
75.
50.
25.
0.1
1.0
10.0
100.0
1000.0
TIME AFTER EMPLACEMENT, t (years)
5b
5a
4
3
2
1

Figure 7d

affecting the mechanical integrity of the rock. The effect of a reduction of the room-to-room distance to 12.5 m is shown in App. II, Table 3. In the case of reprocessed HLW, the repository loading increases from about 25.0% to the maximum 100% as the waste age at emplacement increases from 10.0 years to 89.0 or 98.0 years for emplacement in salt or granite respectively. For spent fuel emplacement in granite, the increase in repository mass loading declines from ~12.0% to ~4.0% as the waste age increases from 10.0 to 100.0 years.

5.2.4 Number of canisters per hole

If two reprocessed HLW canisters are emplaced in each hole, instead of one, the repository mass loading will either increase or decrease depending on the waste age at the time of emplacement. The cross-over occurs at a waste age at emplacement of 35.0 or 49.0 years depending on the geological medium, salt or granite respectively. The results are shown in App. II, Table 4.

* * *

The effects of changes in the various design parameters on the minimal canister pitch as a function of waste age at emplacement are summarized in Figure 8 (a)-(d).

5.3 Variable canister loading

Next, the canister loading was permitted to vary and for each combination of waste age and canister pitch the maximum permissible value of the canister loading for which the backfill temperature limit of 100°C would not be violated was calculated. In these

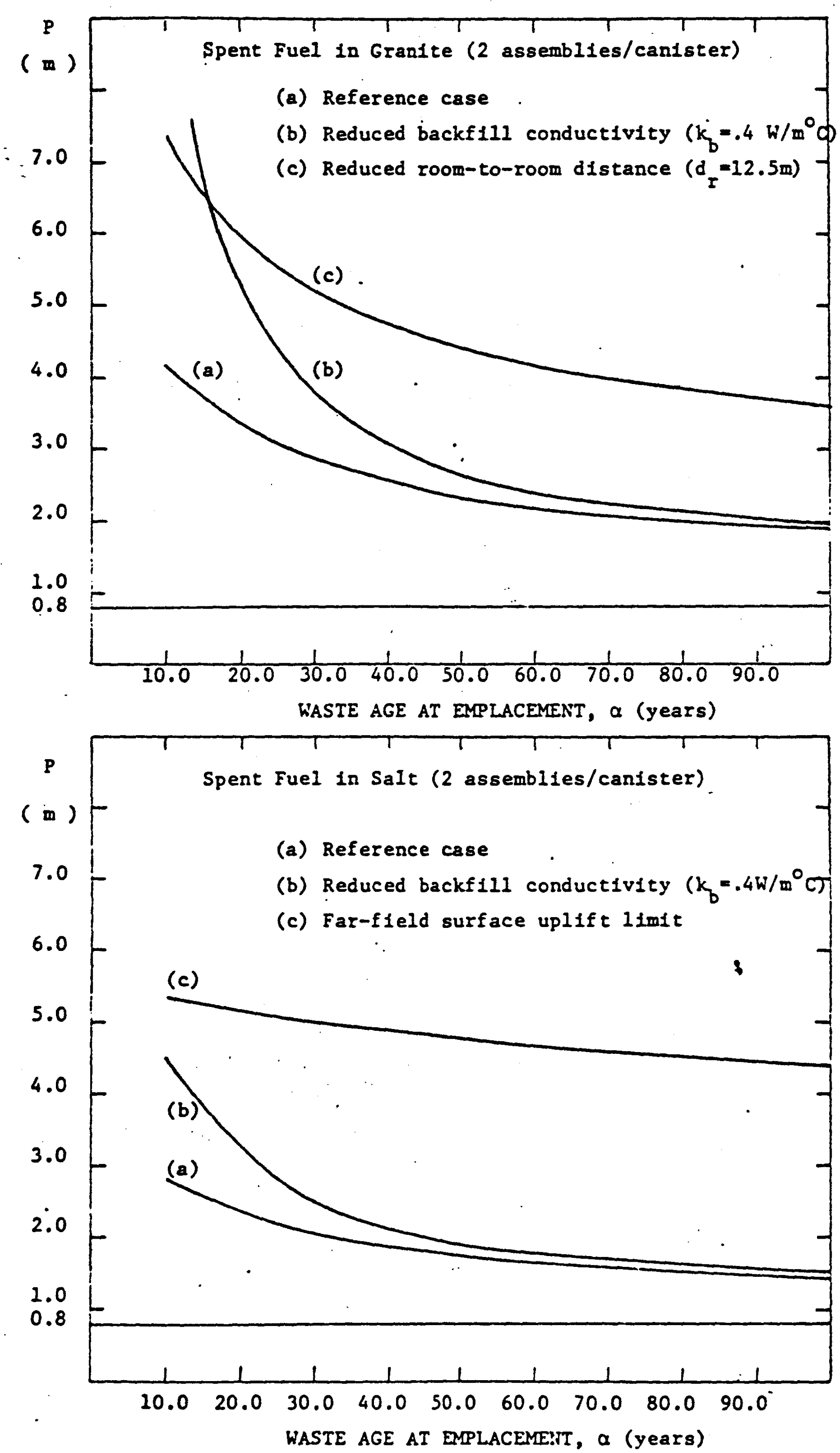
P
(m)
Spent Fuel in Granite (2 assemblies/canister)
(a) Reference case
(b) Reduced backfill conductivity (k_b=.4 W/m°C)
(c) Reduced room-to-room distance (d_r=12.5m)
7.0
6.0
5.0
4.0
3.0
2.0
1.0
0.8
(a)
(b)
(c)
10.0 20.0 30.0 40.0 50.0 60.0 70.0 80.0 90.0
WASTE AGE AT EMPLACEMENT, α (years)
P
(m)
Spent Fuel in Salt (2 assemblies/canister)
(a) Reference case
(b) Reduced backfill conductivity (k_b=.4W/m°C)
(c) Far-field surface uplift limit
7.0
6.0
5.0
4.0
3.0
2.0
1.0
0.8
(a)
(b)
(c)
10.0 20.0 30.0 40.0 50.0 60.0 70.0 80.0 90.0
WASTE AGE AT EMPLACEMENT, α (years)

Figure 8(a)-(b)

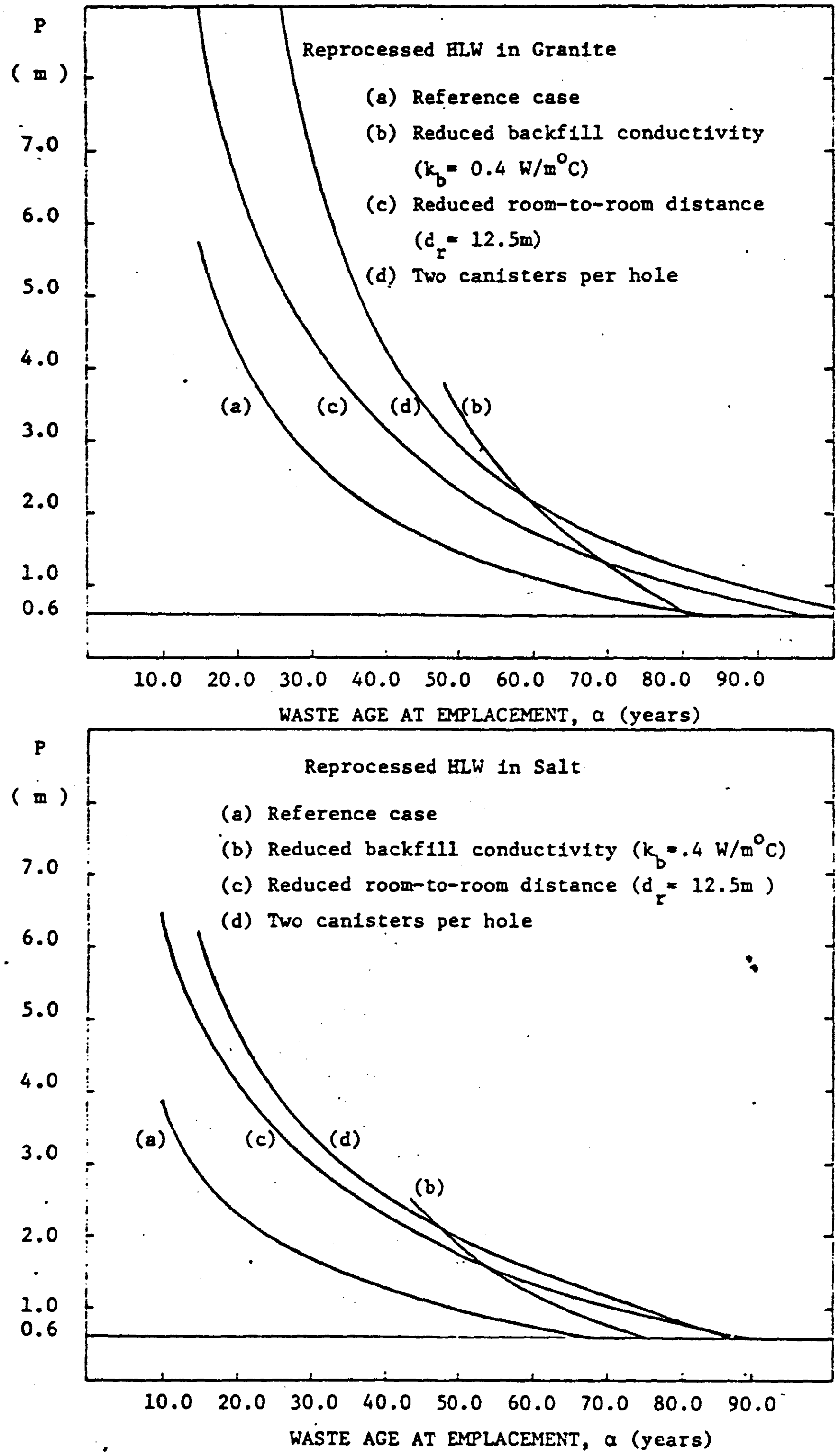
P
(m)
7.0
6.0
5.0
4.0
3.0
2.0
1.0
0.6
Reprocessed HLW in Granite
(a) Reference case
(b) Reduced backfill conductivity
(k_b= 0.4 W/m°C)
(c) Reduced room-to-room distance
(d_r= 12.5m)
(d) Two canisters per hole
(a)
(c)
(d)
(b)
10.0 20.0 30.0 40.0 50.0 60.0 70.0 80.0 90.0
WASTE AGE AT EMPLACEMENT, α (years)
P
(m)
7.0
6.0
5.0
4.0
3.0
2.0
1.0
0.6
Reprocessed HLW in Salt
(a) Reference case
(b) Reduced backfill conductivity (k_b=.4 W/m°C)
(c) Reduced room-to-room distance (d_r= 12.5m)
(d) Two canisters per hole
(a)
(c)
(d)
(b)
10.0 20.0 30.0 40.0 50.0 60.0 70.0 80.0 90.0
WASTE AGE AT EMPLACEMENT, α (years)

Figure 8(c)-(d)

calculations upper limits on the canister loading of 2.4 MTHM for spent fuel (corresponding to the fuel rod close packing limit) and 5.0 MTHM equivalent for reprocessed high-level waste (corresponding to a maximum radionuclide fraction in the waste glass of 30 w/o) are imposed.

Similar calculations were performed for the thermal limits on the rock and the waste matrix. In each case, the corresponding maximum repository mass loading (in kg/m^2 of repository area) was also computed. These results were then compared with the maximum repository mass loading at which the far-field, surface uplift limit would not be violated (figure 4).

Figure 9(a) shows that for spent fuel aged ten years at the time of emplacement in salt, it is the far-field thermal constraint which controls the repository mass loading for values of the canister pitch less than 11 meters. However, for 10-year old reprocessed high-level waste in salt the repository loading is determined by the backfill temperature limit (see figure 9(b)).

The controlling thermal constraint may change as the age of the waste at emplacement increases. Figures 10(a) and 10(b) show, for salt repositories containing spent fuel and reprocessed high-level waste respectively, which thermal constraint dominates and to what extent the repository loading can be expanded as the waste age at emplacement is increased. For spent fuel, the surface uplift limit is the most restrictive of the four thermal criteria over virtually the entire range of values considered for the waste age and canister pitch. Consequently, the maximum permissible repository mass loading is independent of the canister pitch.

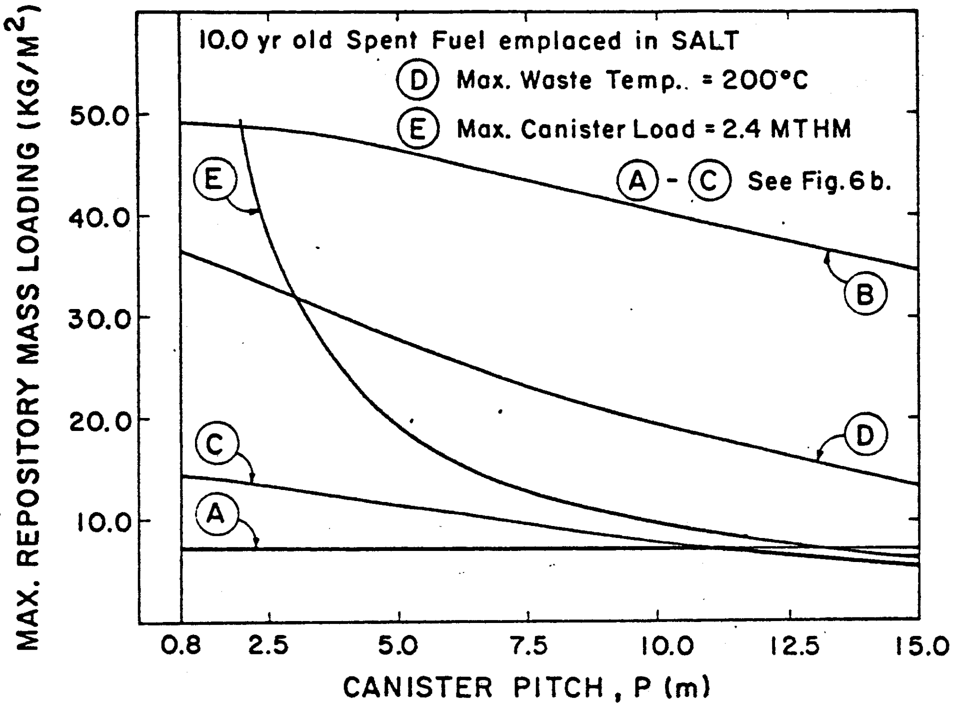

10.0 yr old Spent Fuel emplaced in SALT
D Max. Waste Temp.. = 200°C
E Max. Canister Load = 2.4 MTHM
A - C See Fig. 6 b.
MAX. REPOSITORY MASS LOADING (KG/M²)
50.0
40.0
30.0
20.0
10.0
0.8
2.5
5.0
7.5
10.0
12.5
15.0
CANISTER PITCH, P (m)

FIG. 9(a)

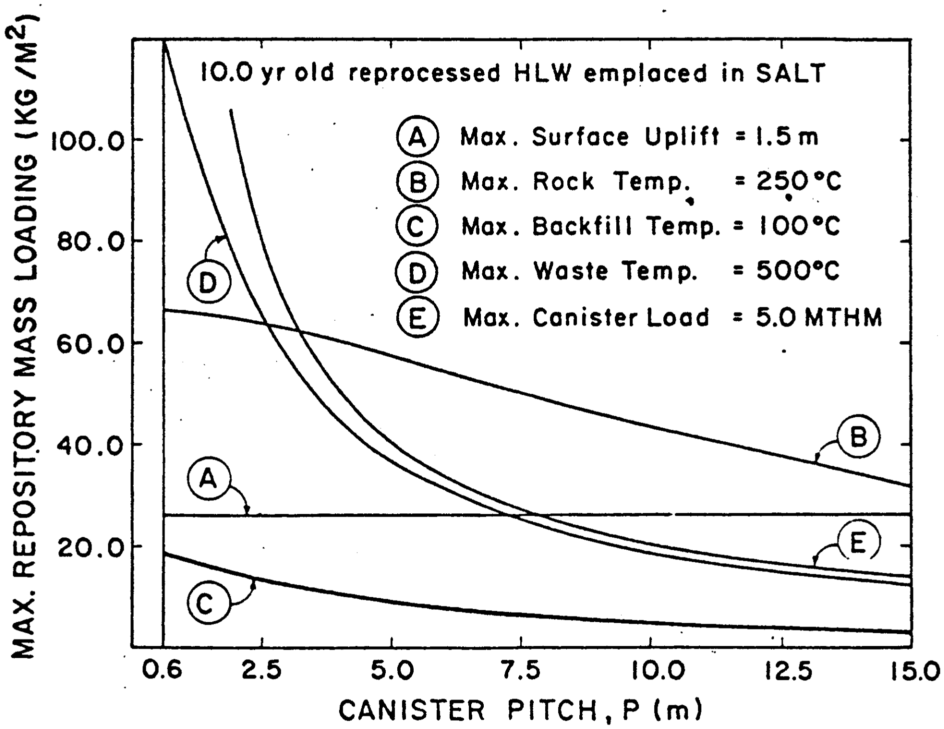

10.0 yr old reprocessed HLW emplaced in SALT
A Max. Surface Uplift = 1.5 m
B Max. Rock Temp. = 250°C
C Max. Backfill Temp. = 100°C
D Max. Waste Temp. = 500°C
E Max. Canister Load = 5.0 MTHM
MAX. REPOSITORY MASS LOADING (KG/M²)
100.0
80.0
60.0
40.0
20.0
0.6
2.5
5.0
7.5
10.0
12.5
15.0
CANISTER PITCH, P (m)

FIG. 9(b)

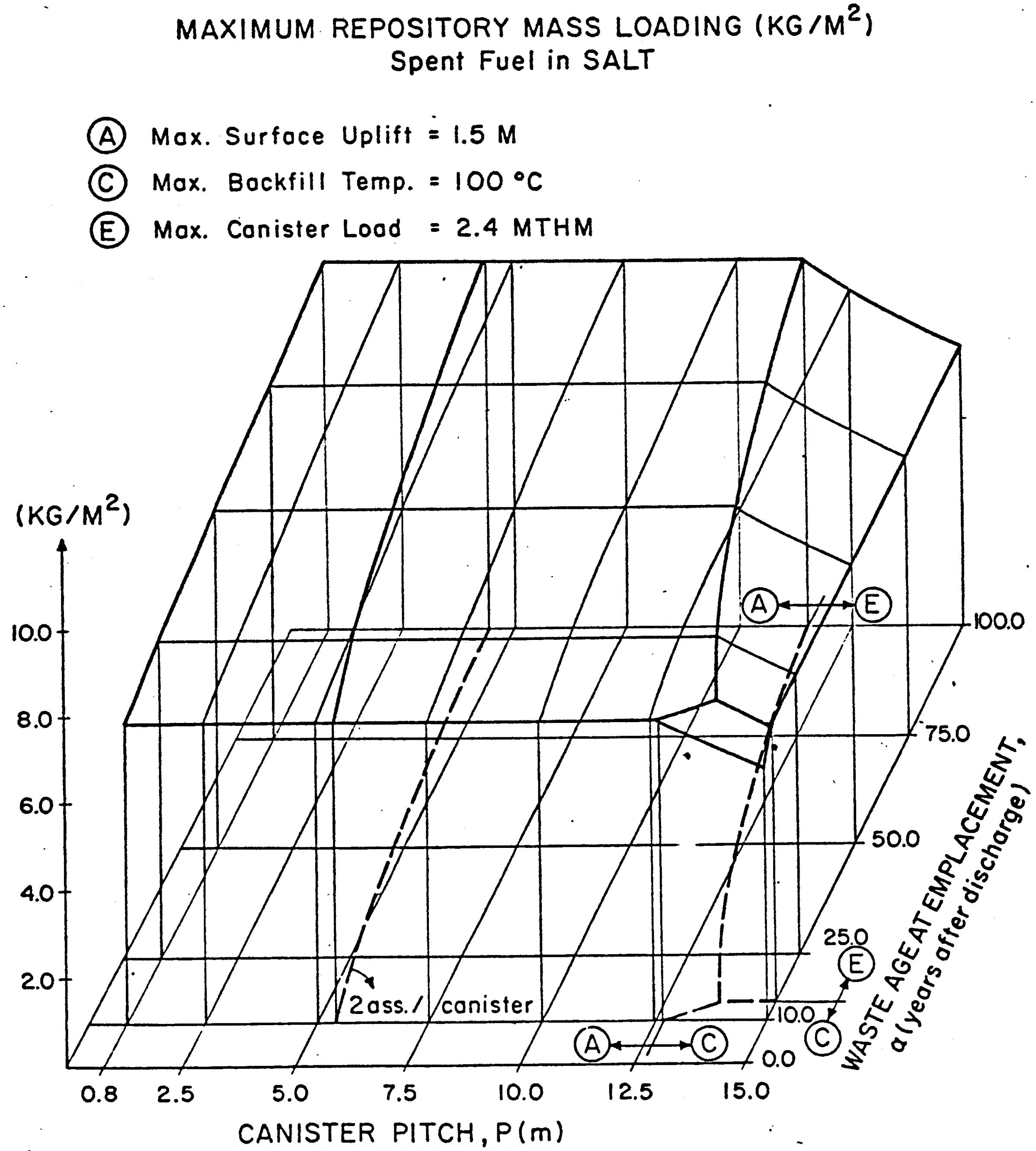
MAXIMUM REPOSITORY MASS LOADING (KG/M²)
Spent Fuel in SALT
(A) Max. Surface Uplift = 1.5 M
(C) Max. Backfill Temp. = 100 °C
(E) Max. Canister Load = 2.4 MTHM
(KG/M²)
10.0
8.0
6.0
4.0
2.0
0.8
2.5
5.0
7.5
10.0
12.5
15.0
CANISTER PITCH, P(m)
100.0
75.0
50.0
25.0
10.0
0.0
WASTE AGE AT EMPLACEMENT, a (years after discharge)
2 ass./ canister
A
C
E

FIG. 10(a)

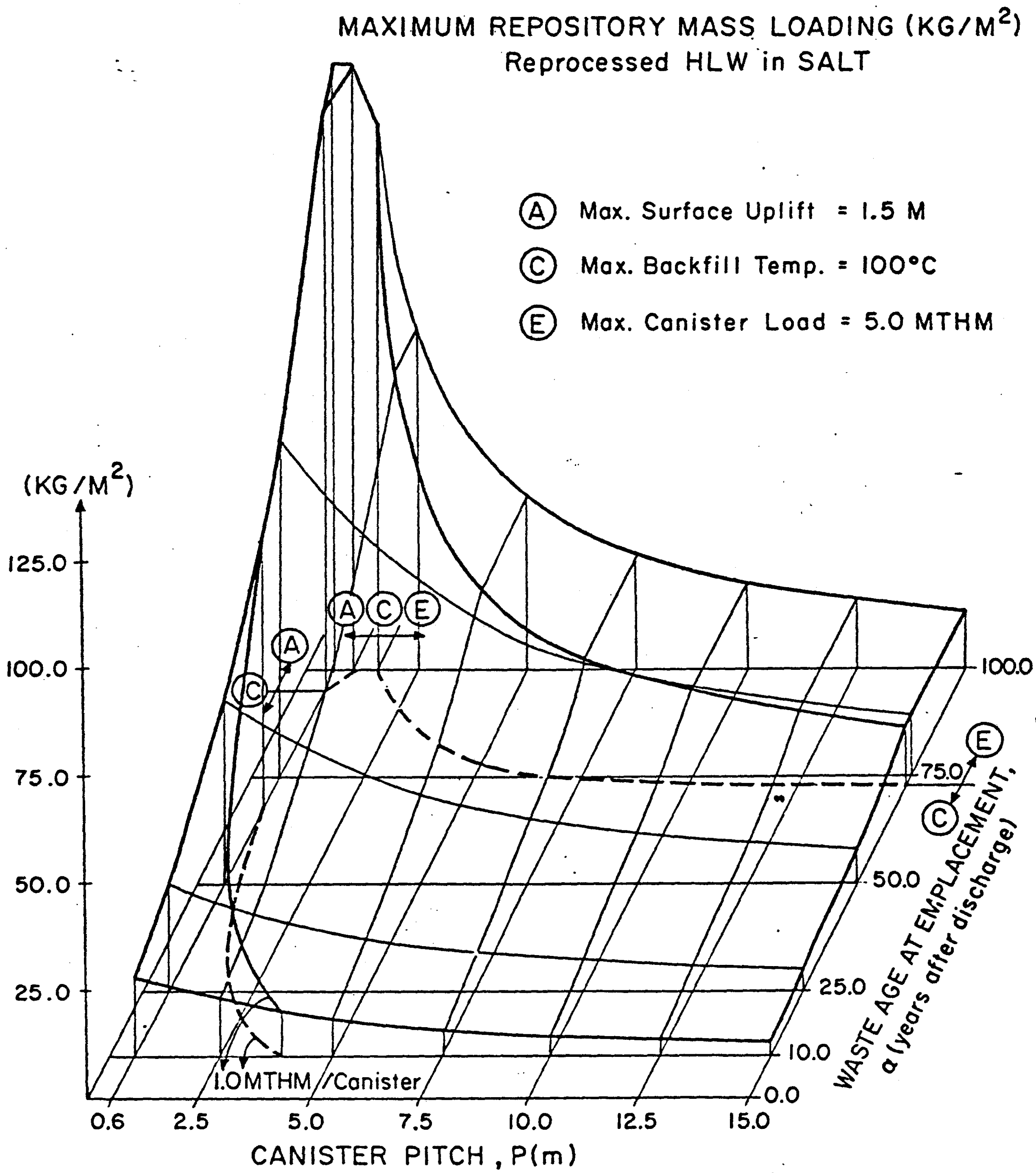
MAXIMUM REPOSITORY MASS LOADING (KG/M2)
Reprocessed HLW in SALT
(A) Max. Surface Uplift = 1.5 M
(C) Max. Backfill Temp. = 100°C
(E) Max. Canister Load = 5.0 MTHM
(KG/M2)
125.0
100.0
75.0
50.0
25.0
1.0MTHM/Canister
0.6
2.5
5.0
7.5
10.0
12.5
15.0
CANISTER PITCH, P(m)
0.0
10.0
25.0
50.0
75.0
100.0
WASTE AGE AT EMPLACEMENT,
α (years after discharge)

FIG. 10(b)

Moreover, it is only weakly dependent on the age of the waste at emplacement, increasing by a factor of 1.22, from 6.87 kg/m^2 to 8.39 kg/m^2, for an increase in the waste age from 10 to 100 years.

By contrast, for reprocessed high-level waste the backfill temperature limit remains the most restrictive criterion for most values of waste age and canister pitch. Furthermore, delay in waste burial greatly increases the allowable repository loading. For example, at a canister pitch of 0.6m (the smallest possible value), when the waste age at emplacement is increased from 10 to 100 years the maximum repository loading increases by a factor of 7.63, from 18.51 kg/m^2 to 141.15 kg/m^2. The much greater sensitivity of the repository loading to the waste age in this case is because of the more rapid thermal decay of the reprocessed high-level waste compared with the spent fuel, once more than about thirty years have elapsed since generation. (It should be noted that no account is taken here of the areal requirements of the low-heat transuranic (TRU) wastes generated during reprocessing, which will most probably also be stored in the repository. The additional areal requirements for the TRU canisters and drums will be approximately 20 m^2/MTHM [7].)

The corresponding results for granite repositories are shown in Figures 10(c) and 10(d).

MAXIMUM REPOSITORY MASS LOADING (KG/M^2)
Spent Fuel in GRANITE

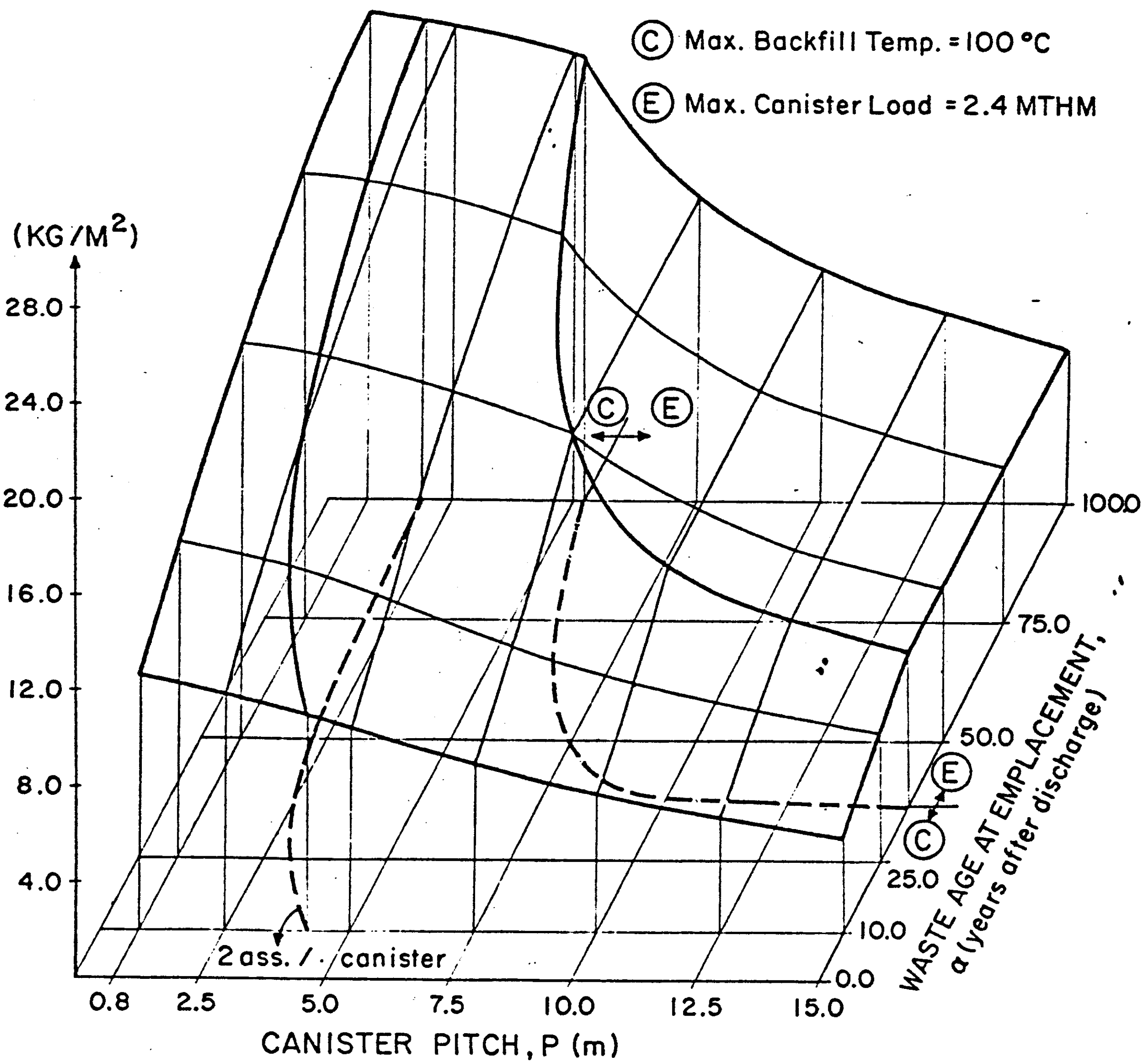

FIG. 10(c)

MAXIMUM REPOSITORY MASS LOADING (KG/M²)
Reprocessed HLW in GRANITE

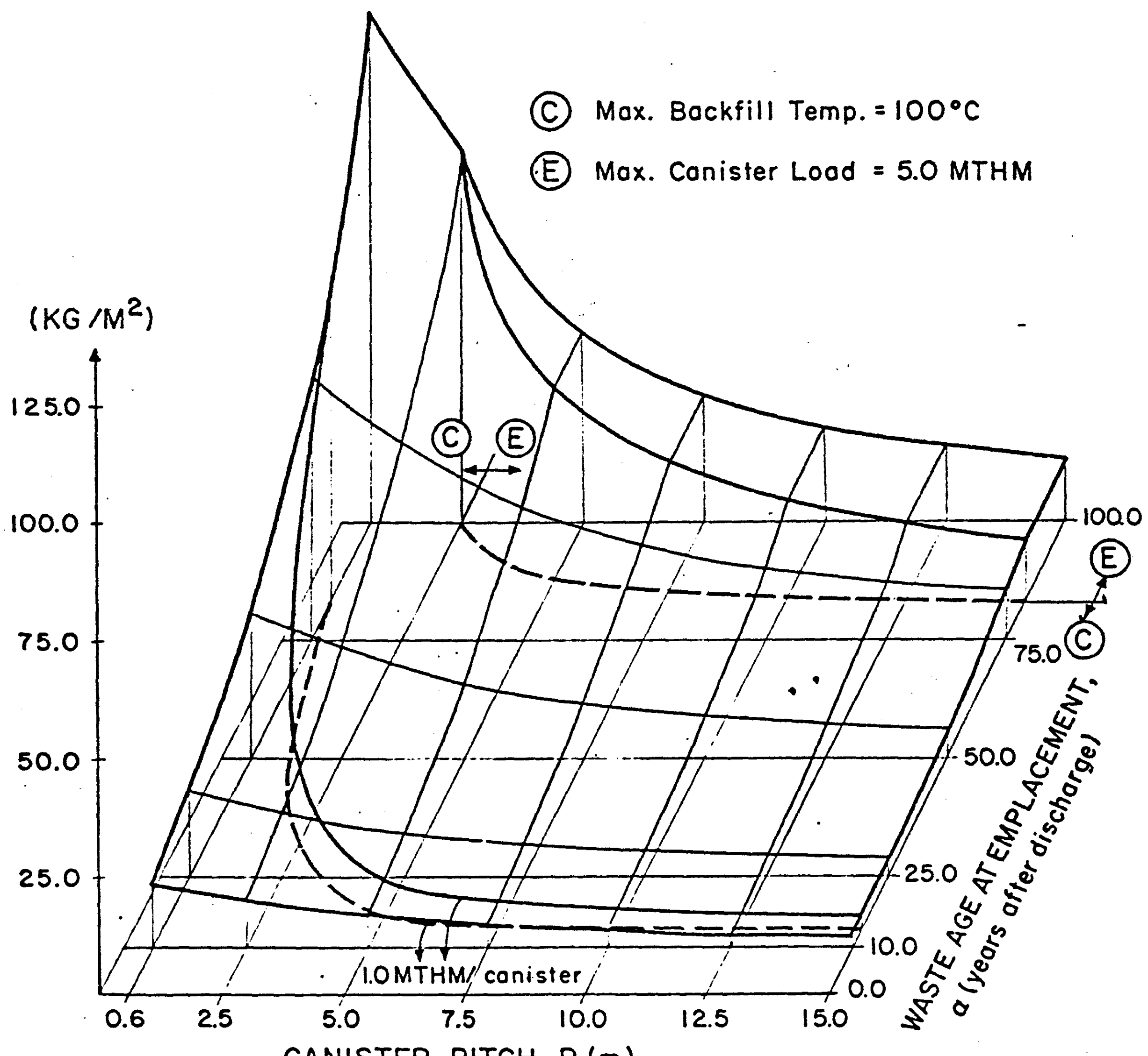

FIG. 10(d)

In Figure 11 (a)-(d) the maximum canister loading is shown as a function of waste age and canister pitch for the four cases considered.

6. Application

The two most important components of the total cost of waste emplacement are the cost of excavation and the waste packaging cost. The former varies inversely with the repository mass loading and the latter varies inversely with the canister loading. An inspection of Figures 10 and 11 indicates that at each value of the waste age at emplacement an optimal canister pitch can be found for which the sum of excavation and packaging costs per unit of waste is minimized. By deferring waste disposal the optimized excavation and packaging unit costs both decline, but the unit cost of interim storage is increased. With the appropriate cost data, the interim waste storage period which results in the minimum overall system cost can be determined. In future work, the simplified repository thermal model presented here will be used to address the economic optimization problem.

7. Conclusions

An approximate, semi-analytical model for predicting the time-dependent temperature distribution in the region of a high-level waste repository has been developed. The model has been applied to a determination of the maximum permissible repository average mass loading and canister loading for spent PWR fuel and reprocessed PWR high-level waste repositories in salt and granite media, subject to several independent thermal constraints. The impact of these constraints on key repository design parameters has been investigated

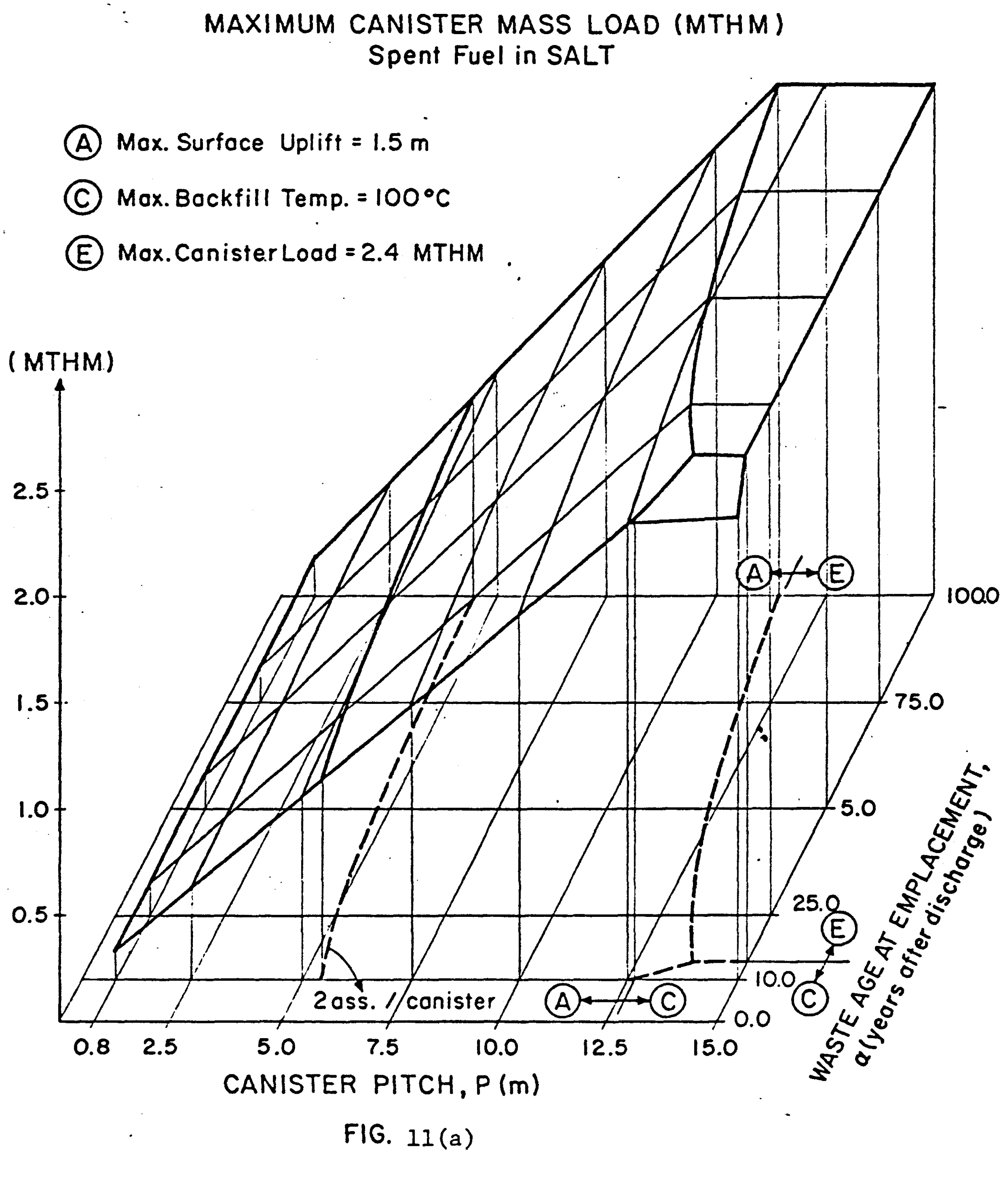
MAXIMUM CANISTER MASS LOAD (MTHM)
Spent Fuel in SALT
(A) Max. Surface Uplift = 1.5 m
(C) Max. Backfill Temp. = 100°C
(E) Max. Canister Load = 2.4 MTHM
(MTHM)
2.5
2.0
1.5
1.0
0.5
0.8
2.5
5.0
7.5
10.0
12.5
15.0
CANISTER PITCH, P (m)
2 ass. / canister
(A)
(C)
(E)
100.0
75.0
5.0
25.0
10.0
0.0
WASTE AGE AT EMPLACEMENT,
α (years after discharge)

FIG. 11(a)

MAXIMUM CANISTER MASS LOADING (KGHM)
Reprocessed HLW in SALT

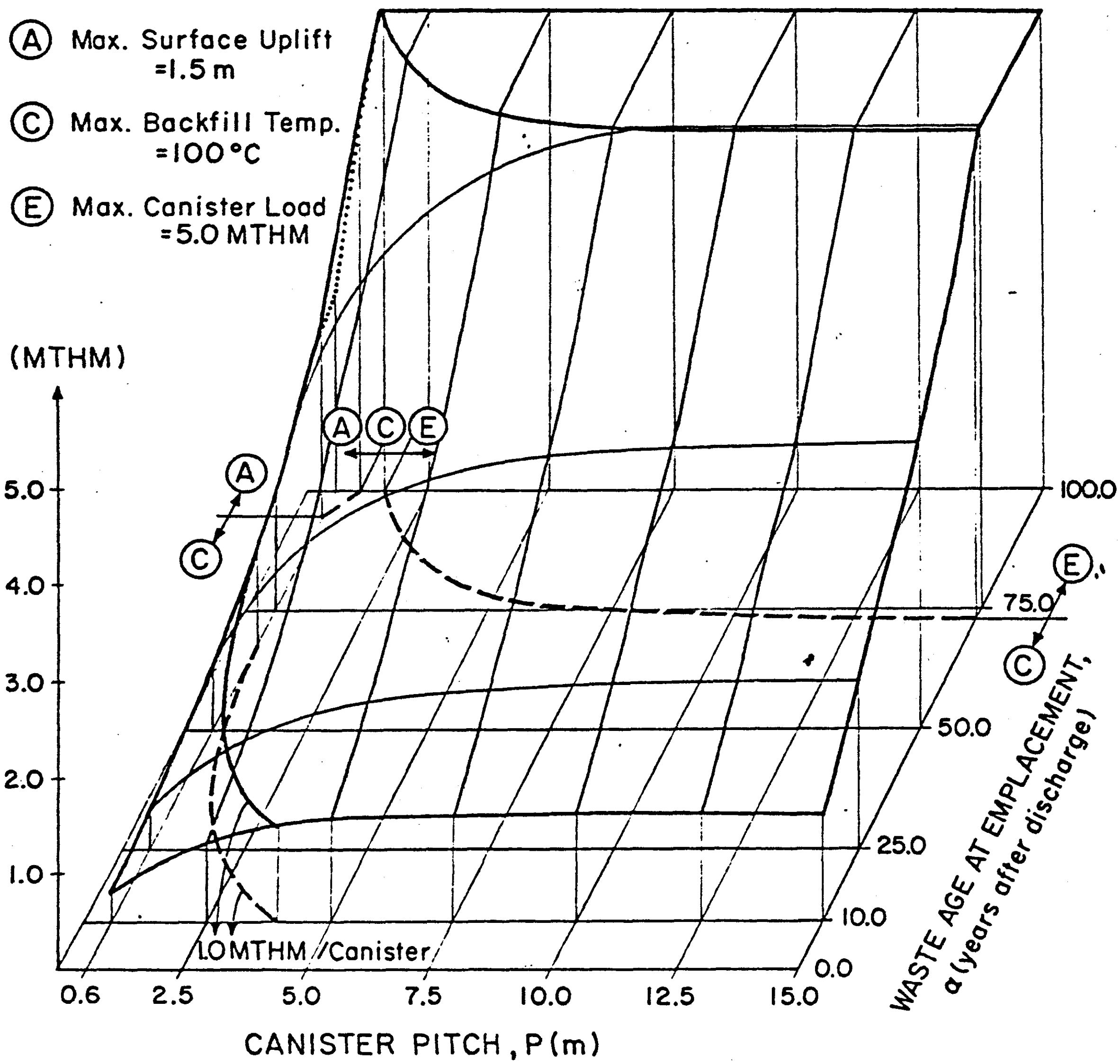

FIG. 11(b)

MAXIMUM CANISTER MASS LOADING (MTHM)
Spent Fuel in GRANITE

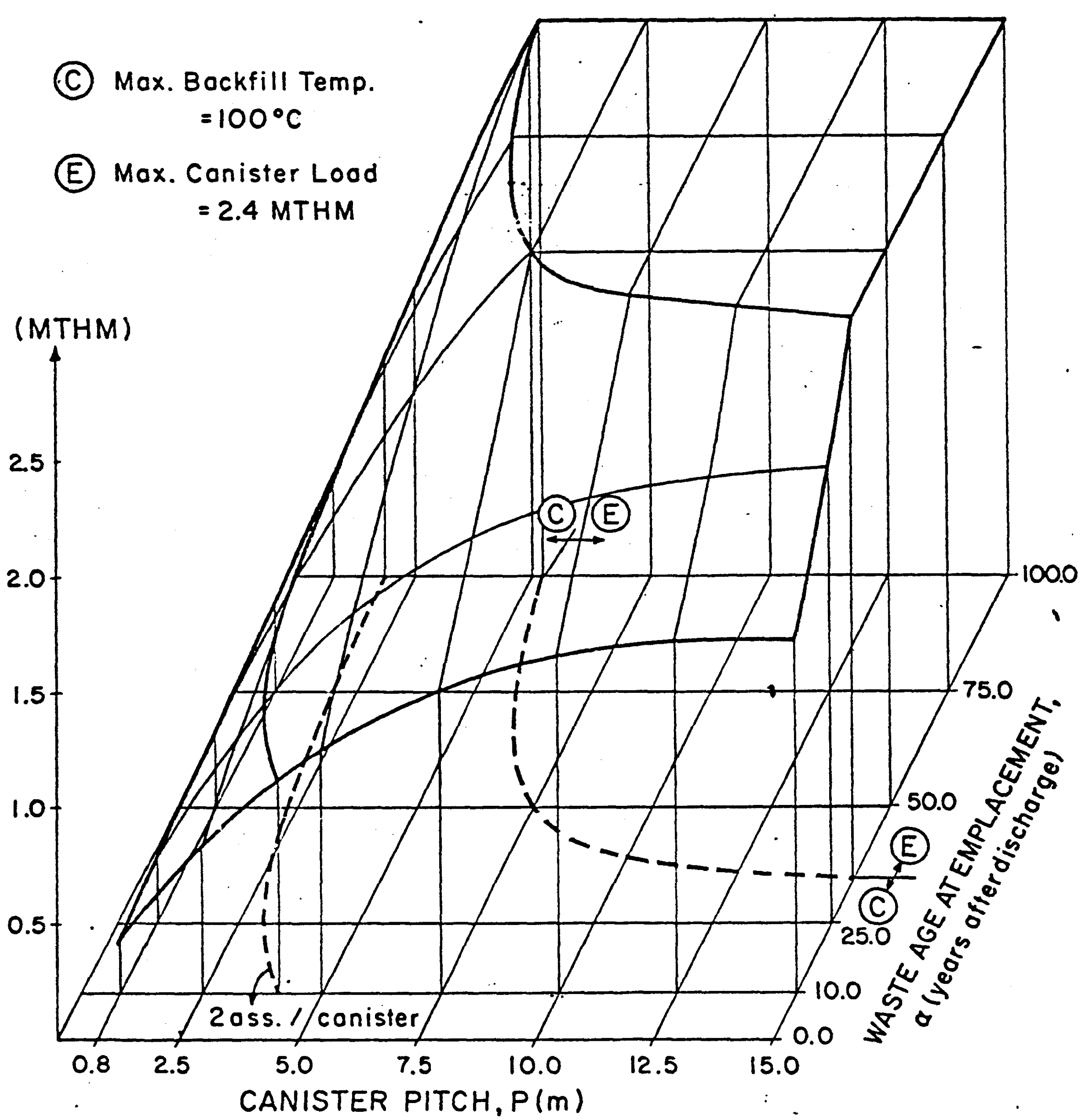

FIG. 11(c)

MAXIMUM CANISTER MASS LOADING (MTHM)
Reprocessed HLW in GRANITE

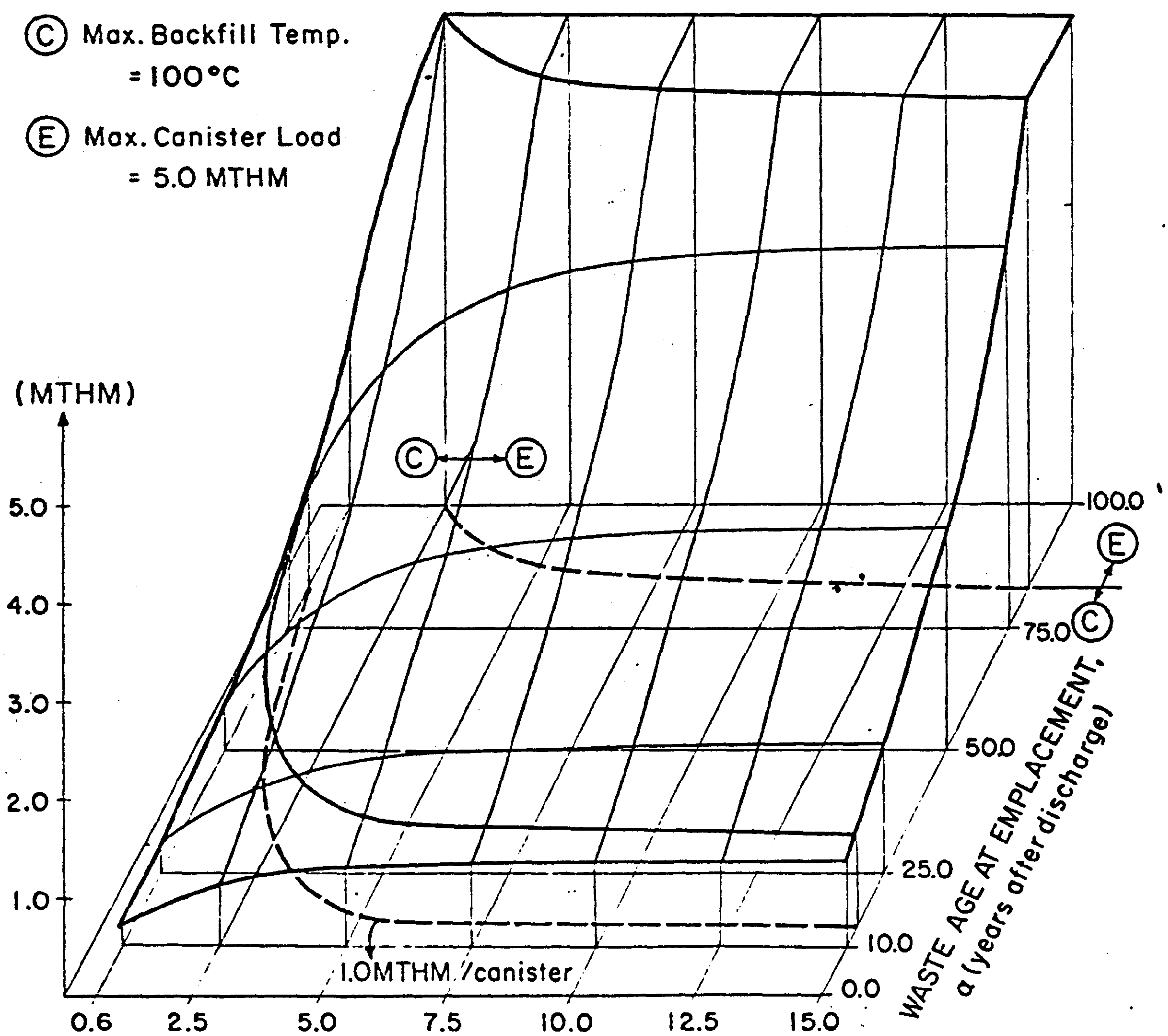

FIG. 11(d)

for values of the waste age at emplacement ranging from 10 to 100 years. It is found that for spent fuel repositories in salt the surface uplift criterion determines the maximum permissible repository mass loading, while in the other three cases both the repository loading and the canister loading are controlled by the bentonite backfill temperature constraint. Finally, despite the differences between the thermal and thermoeleastic properties of salt and granite, neither medium appears to offer decisive advantages in terms of the maximum permissible waste loading in the repository.

Acknowledgement

This work was supported by the U.S. Department of Energy, under Contract EX-76-A-01-2295.

References

[1] U.S. Department of Energy, Final Environmental Impact Statement: Management of Commercially Generated Radioactive Waste, DOE/EIS-0046F (October 1980), App. K.

[2] W.D. Turner, D.C. Elrod and I.I. Siman-Tov, HEATING 5 - An IBM 360 heat conduction program, Oak Ridge National Laboratory Report, ORNL/CSD/TM-15 (March 1977).

[3] W.M. Kays, F. Hossaini-Hashemi, and J.S. Busch, Calculation of media temperatures for nuclear sources in geologic depositories by a finite-length line source superposition model (FLLSSM), Nucl. Engrg. Des. 67 (1981), 339-347.

[4] P.-E. Ahlström, Ceramic and pure-metal canisters in buffer material for high level radioactive waste, Nuclear and Chemical Waste Management 1 (1980) 77-88.

[5] C.M. Malbrain, R.K. Lester and J.M. Deutch, Analytical approximations for the long-term decay behaviour of spent fuel and high-level waste, Nucl. Tech. 57 (1982).

[6] J.E. Russell, Areal thermal loading recommendations for nuclear waste repository in salt, Union Carbide Corporation Report, Office of Waste Isolation, Y/OWI/TM-37 (1977).

[7]. International Atomic Energy Agency, International Nuclear Fuel Cycle Evaluation, Volume 7: Waste Management and Disposal (1980).

[8] M.H. Tennant, Sensitivity calculations for low-heat generating defense waste repository temperatures, Nucl. Engrg. Des. 67 (1981) 391-396.

Appendix I: Illustration of Some of the Near-Field Model Assumptions

Table A.I.-1: Reprocessed HLW in Salt
Single heat source (model assumptions i-4)

Maximum salt temperature increase for alternative heat source models as a function of the radial distance from the source centerline, at the source midplane.

r (m)	$\Delta T_{1,max}$ (^oC)	$\Delta T_{2,max}$ (^oC)	$\Delta T_{3,max}$ (^oC)	$t_{i,max}$ (yrs)
0.0	--	49.12	49.13	0.32
0.2	39.80	39.50	39.75	0.32
0.3	33.60	33.55	33.47	0.32
1.0	16.57	16.59	15.17	1.0
2.0	9.13	9.14	4.89	1.0
5.0	3.38	3.38	<0	3.16

Waste age at emplacement,	α	=	10.0 yrs
Canister waste loading,	M_c	=	2.0 MTHM
Active canister length,	L_c	=	3.0 m
Active canister radius,	R_c	=	0.18 m
Equivalent active canister width,	W_c	=	0.316m

Table A.I-1 (continued)

Model 1: Finite length line heat source

$$\Delta T_1(r,t) = \frac{1}{4\pi D L_c} \int_0^t \frac{Q_c(t+\alpha-\tau)}{\tau} \cdot e^{-r^2/4D\tau} \cdot \operatorname{erf} \frac{L_c}{4\sqrt{D\tau}} \, d\tau \qquad (A.1)$$

Model 2: Parallellepiped heat source

$$\Delta T_2(r,t) = \frac{1}{2W_c^2 L_c} \int_0^t Q_c(t+\alpha-\tau) \left\{ \operatorname{erf} \frac{r+W_c/2}{\sqrt{4D\tau}} - \operatorname{erf} \frac{r-W_c/2}{\sqrt{4D\tau}} \right\} \operatorname{erf} \frac{W_c}{4\sqrt{D\tau}} \cdot \operatorname{erf} \frac{L_c}{4\sqrt{D\tau}} \, d\tau \qquad (A.2)$$

Model 3: Cylindrical heat source

$$\Delta T_3(r,t) = \frac{1}{\pi R_c^2 L_c} \int_0^t Q_c(t+\alpha-\tau) \left\{ 1-e^{-R_c^2/4D\tau} \right\} \cdot \operatorname{erf} \frac{L_c}{4\sqrt{D\tau}} \, d\tau$$

$$\begin{cases} -\dfrac{Q_c(t+\alpha)}{4\pi D L_c} \left\{ \dfrac{r}{R_c} \right\}^2 \text{ for } r \leq R_c & (A.3) \\[2ex] -\dfrac{Q_c(t+\tau)}{4\pi D L_c} \left\{ 1 + 2 \ln \dfrac{r}{R_c} \right\} \text{ for } r > R_c & (A.3') \end{cases}$$

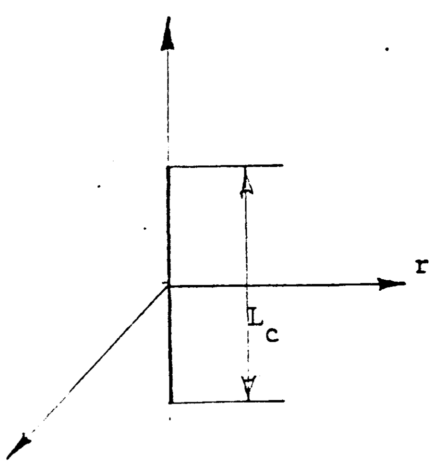

Model 1

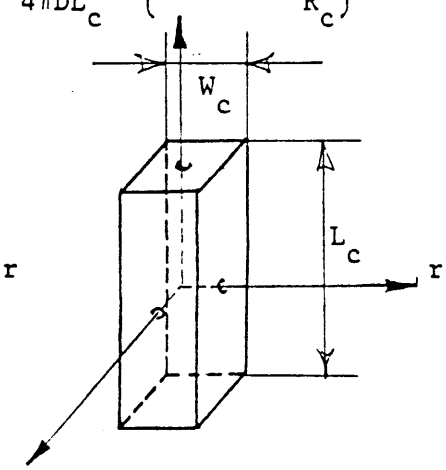

Model 2

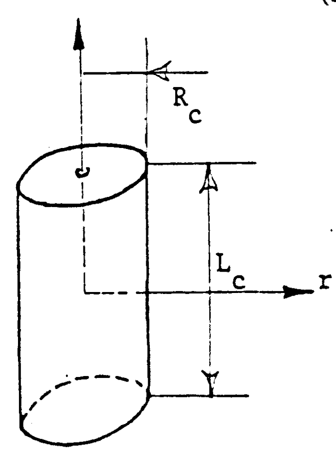

Model 3

Table A.II.-2: Reprocessed HLW in Salt
Infinite row of canisters (model assumption viii)

Maximum salt temperature increase at the repository midplane as a function of the distance from the center of the disposal room for two different source models.

y (m)	$\Delta T_{1,max}$ (^oC)	$\Delta T_{2,max}$ (^oC)	$t_{1,max}$ (^oC)	$t_{2,max}$ (^oC)
0.0	25.55	50.79	10.0	3.16
12.5	18.47	15.72	10.0	10.0
25.0	11.15	10.85	31.62	31.62
50.0	6.08	6.00	31.62	31.62
75.0	3.56	3.56	100.0	100.0

Waste age at emplacement, α = 10.0 yrs

Single canister mass loading, M_c = 2.0 MTHM

Average repository mass loading, M = 25.90 kg/m^2

Active canister length, L_c = 3.0 m

Distance between adjacent rooms, d_r = 25.0 m

Distance between adjacent canisters, P_c = 3.09 m

Table A.II.-2 (Continued)

Model 1: Infinitely long parallelepiped heat source

$$\Delta T_1(y,t) = \frac{1}{2d_r P_c L_c} \int_0^t Q_c(t+\alpha-\tau)\left\{\text{erf}\,\frac{y+d_r/2}{\sqrt{4D\tau}} - \text{erf}\,\frac{y-d_r/2}{\sqrt{4D\tau}}\right\} \cdot \text{erf}\,\frac{L_c}{4\sqrt{D\tau}}\, d\tau \qquad (A.4)$$

Model 2: Infinitely long parallelepiped heat source

$$\Delta T_2(y,t) = \frac{1}{2W_c P_c L_c} \int_0^t Q_c(t+\alpha-\tau)\left\{\text{erf}\,\frac{y+W_c/2}{\sqrt{4D\tau}} - \text{erf}\,\frac{y-W_c/2}{\sqrt{4D\tau}}\right\} \cdot \text{erf}\,\frac{L_c}{4\sqrt{D\tau}}\, d\tau \qquad (A.5)$$

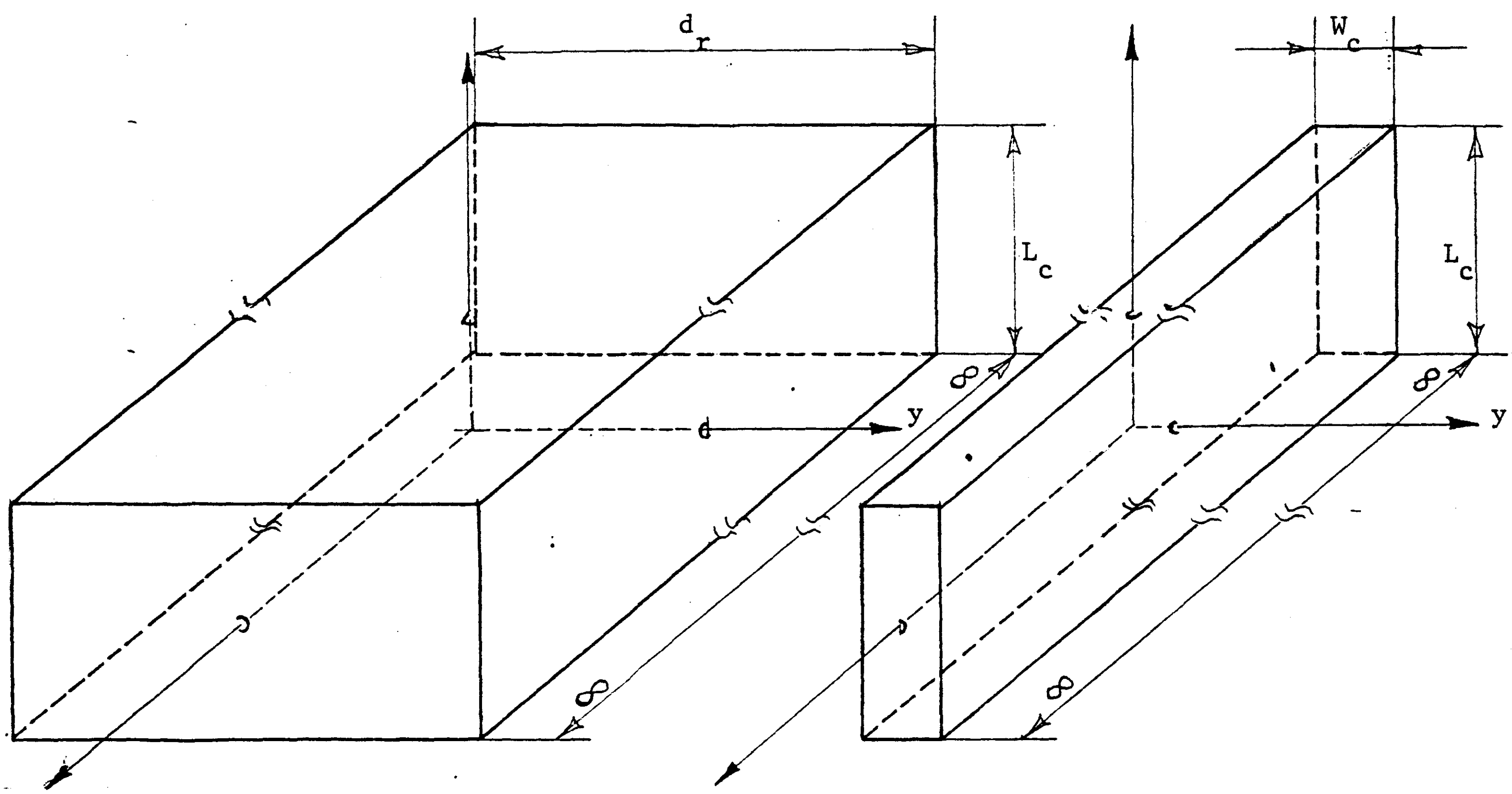

Model 1 Model 2

Table A.I.-3: Reprocessed HLW in Salt
Finite row of canisters (model assumption ix)

Maximum salt temperature increase at the repository midplane as a function of the distance from the center of the disposal room for different room lengths.

y (m)	$\Delta T_{1,max}$ (°C)	$\Delta T_{2,max}$ (°C)	$\Delta T_{3,max}$ (°C)	$\Delta T_{4,max}$ (°C)	$\Delta T_{5,max}$ (°C)	$t_{5,max}$ (yrs)
0.0	50.65	50.78	50.79	50.79	50.79	3.16
12.5	14.55	15.66	15.72	15.72	15.72	10.0
25.0	7.96	10.16	10.84	10.85	10.85	31.62
50.0	3.88	5.45	6.00	6.00	6.00	31.62
75.0	1.36	2.97	3.44	3.56	3.56	100.0
L_r (m)	100.0	200.0	500.0	1000.0	∞	

Waste age at emplacement,	α	= 10.0 yrs
Single canister mass loading,	M_c	= 2.0 MTHM
Average repository mass loading,	M	= 25.90 kg/m^2
Active canister length,	L_c	= 3.0 m
Distance between adjacent rooms,	d_r	= 25.0 m
Distance between adjacent canisters,	P_c	= 3.09 m

Table A.I.-3 (Continued)

Model : parallelepiped heat source

$$\Delta T(y,t) = \frac{1}{2W_c P_c L_c} \int_0^t Q_c(t+\alpha-\tau)\left\{ \mathrm{erf}\frac{y+W_c/2}{\sqrt{4D\tau}} - \mathrm{erf}\frac{y-W_c/2}{\sqrt{4D\tau}}\right\} \cdot \left\{ \mathrm{erf}\frac{L_r}{4\sqrt{D\tau}}\right\} \cdot \left\{ \mathrm{erf}\frac{L_c}{4\sqrt{D\tau}}\right\} d\tau \qquad (A.6)$$

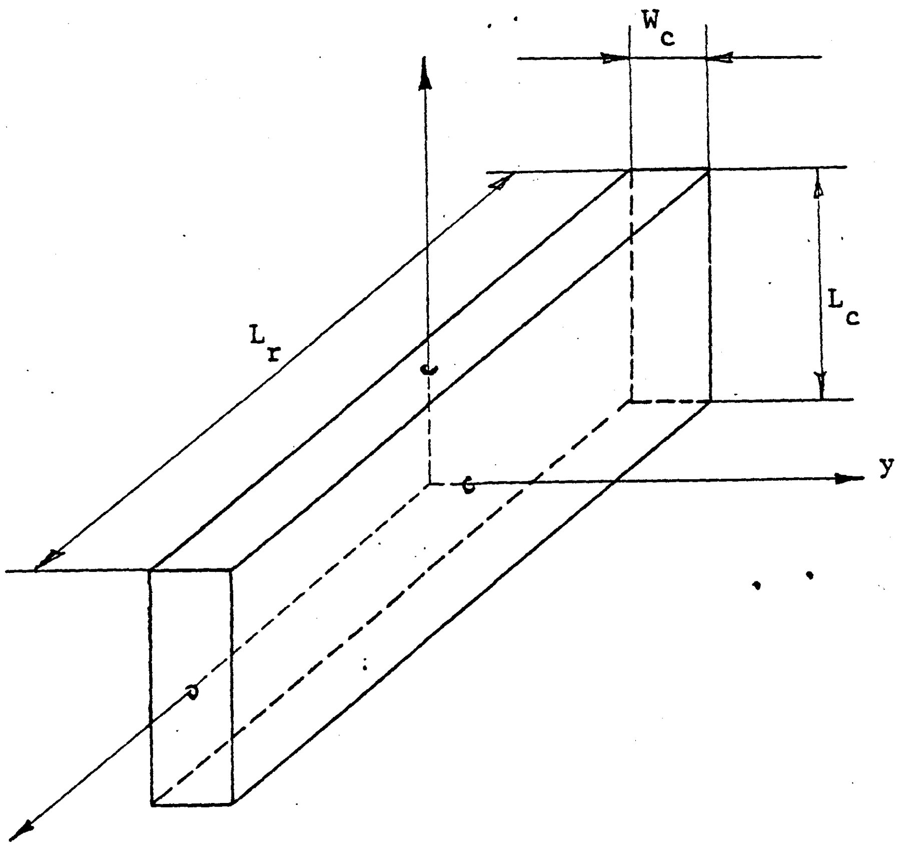

Table A.I.-4: Reprocessed HLW in Salt
Single heat source (model assumption x)

x (m)	$\Delta T_{1,max}$ (^oC)	$\Delta T_{2,max}$ (^oC)	$\Delta T_{3,max}$ (^oC)	$t_{i,max}$ (yrs)
0.0	5.52	9.69	-	1.0
10.0	1.12	1.33	1.47	3.16
25.0	0.39	0.41	0.42	10.0
50.0	0.14	0.15	0.15	31.62
75.0	0.07	0.07	0.07	31.62

Waste age at emplacement, α = 10.0 yrs

Single canister mass loading, M_c = 2.0 MTHM

Active canister length, L_c = 3.0 m

Average repository mass loading, M = 25.90 kg/m^2

Distance between adjacent rooms, $d_{r1,2}$ = 25.0/12.5 m

Distance between adjacent canisters, $P_{c1,2}$ ≐ 3.09/6.18 m

Table A.I-4 (Continued)

Model 1,2: parallelepiped heat source

$$\Delta T_{1,2}(x,t) = \frac{1}{2d_r P_c L_c} \int_0^t Q_c(t+\alpha-\tau) \cdot \left\{ \mathrm{erf} \frac{x+P_c/2}{\sqrt{4D\tau}} - \mathrm{erf} \frac{x-P_c/2}{\sqrt{4D\tau}} \right\} \cdot \left\{ \mathrm{erf} \frac{d_r}{4\sqrt{D\tau}} \right\} \cdot \left\{ \mathrm{erf} \frac{L_c}{4\sqrt{D\tau}} \right\} d\tau \tag{A.8}$$

Model 3: Single Finite Length Line Heat Source

$$\Delta T_3(x,t) = \frac{1}{4\pi D L_c} \int_0^t Q_c(t+\alpha-\tau) \frac{e^{-x^2/4D\tau}}{\tau} \mathrm{erf} \frac{L_c}{4\sqrt{D\tau}} d\tau \tag{A.9}$$

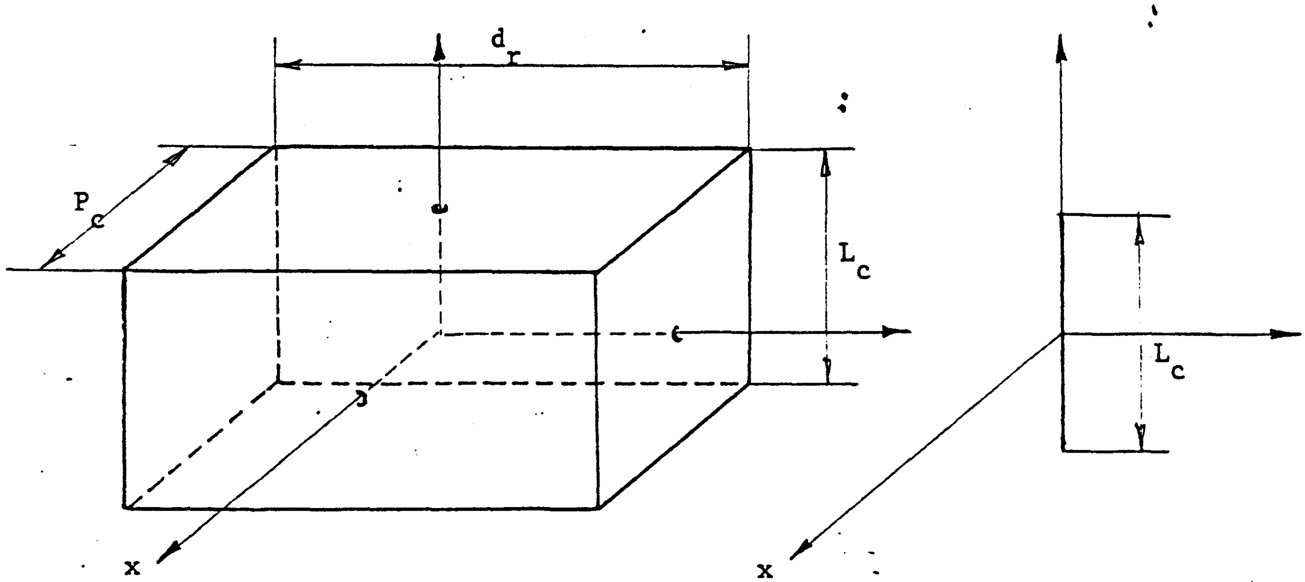

Model 1,2

Model 3

Appendix II: Sensitivity of Repository Mass Loadings to Repository Design Parameters

Table A.II.-1: Reduction in backfill conductivity from 1.2 W/m°C to 0.4 W/m°C

A.II.-1(a): Spent Fuel in Salt

α (yrs)	P (m)	P* (m)	M (kg/m^2)	M* (kg/m^2)	ΔM/M %
10.0	2.85	4.57	12.95	8.07	-37.68
15.0	2.56	3.88	14.42	9.52	-33.98
25.0	2.19	2.79	16.84	13.24	-21.38
50.0	1.76	1.91	21.02	19.28	- 8.28
75.0	1.56	1.65	23.70	22.42	- 5.40
100.0	1.43	1.50	25.79	24.69	- 4.27

A.II.-1(b): Reprocessed HLW in Salt

α (yrs)	P (m)	P* (m)	M (kg/m^2)	M* (kg/m^2)	ΔM/M %
10.0	3.88	-	10.32	-	-100.0
15.0	2.79	-	14.34	-	-100.0
25.0	1.97	-	20.30	-	-100.0
50.0	0.99	1.83	40.40	21.86	- 45.89
75.0	0.60	0.62	66.67	64.14	- 3.79
100.0	0.60	0.60	66.67	66.67	0.0

Table A.II-1 (continued): Reduction in backfill conductivity from 1.2 W/m°C to 0.4 W/m°C

A.II-1(c): Spent Fuel in Granite

α (yrs)	P (m)	P* (m)	M (kg/m²)	M* (kg/m²)	ΔM/M %
10.0	4.13	-	8.93	-	-100.0
15.0	3.73	6.81	9.89	5.42	- 45.20
25.0	3.02	4.40	12.24	8.40	- 31.37
50.0	2.31	2.58	15.97	14.29	- 10.52
75.0	2.02	2.16	18.26	17.08	- 6.46
100.0	1.86	1.94	19.88	19.00	- 4.43

A.II-1(d): Reprocessed HLW in Granite

α (yrs)	P (m)	P* (m)	M (kg/m²)	M* (kg/m²)	ΔM/M %
10.0	-	-	-	-	-
15.0	5.73	-	6.98	-	-100.0
25.0	3.38	-	11.83	-	-100.0
50.0	1.47	3.36	27.28	11.91	- 56.34
75.0	0.73	0.94	54.93	42.37	- 22.87
100.0	0.60	0.60	66.67	66.67	0.0

Table A.II.-2: Introduction of a 25.0 year waiting period prior to hole backfilling

A.II.-2(a): Reprocessed HLW in Salt

α (yrs)	P (m)	P* (m)	M (kg/m^2)	M* (kg/m^2)	ΔM/M (%)
10.0	3.88	3.08	10.32	12.99	+25.84
15.0	2.79	2.45	14.34	16.33	+13.85
25.0	1.97	1.72	20.30	23.26	+14.56
50.0	0.99	0.87	40.40	45.98	+13.80
75.0	0.60	0.60	66.67	66.67	0.0
100.0	0.60	0.60	66.67	66.67	0.0

A.II.-2(b): Reprocessed HLW in Granite

α (yrs)	P (m)	P* (m)	M (kg/m^2)	M* (kg/m^2)	ΔM/M (%)
10.0	-	5.15	-	7.77	∞
15.0	5.73	4.15	6.98	9.64	+38.09
25.0	3.38	2.90	11.83	13.79	+16.59
50.0	1.47	1.28	27.28	31.25	+14.55
75.0	0.73	0.68	54.93	58.82	+ 6.62
100.0	0.60	0.60	66.67	66.67	0.0

Table A.II.-3: Reduction in room-to-room distance by factor of two.

A.II.-3(a): Reprocessed HLW in Salt

α (yrs)	P (m)	P* (m)	M (kg/m^2)	M* (kg/m^2)	ΔM/M (%)
10.0	3.88	6.45	10.32	12.41	+ 20.25
15.0	2.79	4.97	14.34	16.11	+ 12.34
25.0	1.97	3.47	20.30	23.07	+ 13.65
50.0	0.99	1.72	40.40	46.51	+ 15.12
75.0	0.60	0.87	66.67	92.35	+ 38.52
100.0	0.60	0.60	66.67	133.33	+100.0 (1)

A.II.-3(b): Reprocessed HLW in Granite

α (yrs)	P (m)	P* (m)	M (kg/m^2)	M* (kg/m^2)	ΔM/M (%)
10.0	-	-	-	-	-
15.0	5.73	8.98	6.98	8.91	+ 27.65
25.0	3.38	5.30	11.83	15.10	+ 27.64
50.0	1.47	2.34	27.28	34.20	+ 25.37
75.0	0.73	1.15	54.93	69.49	+ 26.51
100.0	0.60	0.60	66.67	133.33	+100.0 (2)

Table A.II.-3 (continued): Reduction in room-to-room distance by a factor of two.

A.II.-3(c): Spent Fuel in Granite(3)

α (yrs)	P (m)	P* (m)	M (kg/m^2)	M* (kg/m^2)	ΔM/M (%)
10.0	4.13	7.40	8.93	9.98	+11.76
15.0	3.73	6.54	9.89	11.28	+14.05
25.0	3.02	5.49	12.24	13.44	+ 9.80
50.0	2.31	4.38	15.97	16.87	+ 5.64
75.0	2.02	3.88	18.26	19.01	+ 4.11
100.0	1.86	3.57	19.88	20.67	+ 3.97

(1) The 100.0% increase in repositing mass loading is attained for waste ages at emplacement greater than 89.0 years.

(2) The 100.0% increase in repository mass loading is attained for waste ages at emplacement greater than 98.0 years.

(3) Spent Fuel emplacement in Salt is not considered. In that case, the far-field surface uplift constraint will determine the repository lay-out.

Table A.II.-4: Emplacement of two canisters per hole

A.II.-4(a): Reprocessed HLW in Salt

α (yrs)	P (m)	P* (m)	M (kg/m^2)	M* (kg/m^2)	ΔM/M (%)
10.0	3.88	-	10.32	-	-100.0
15.0	2.79	6.17	14.34	12.96	- 9.62
25.0	1.97	4.02	20.30	19.89	- 2.02
50.0	0.99	1.93	40.40	41.44	(1) + 2.57
75.0	0.60	0.97	66.67	82.57	+ 23.85
100.0	0.60	0.60	66.67	133.33	+100.0

A.II.-4(b): Reprocessed HLW in Granite

α (yrs)	P (m)	P* (m)	M (kg/m^2)	M* (kg/m^2)	ΔM/M (%)
10.0	-	-	-	-	-
15.0	5.73	-	6.98	-	-100.0
25.0	3.38	9.55	11.83	8.37	- 29.25
50.0	1.47	2.89	27.28	27.64	(2) + 1.32
75.0	0.73	1.39	54.93	57.37	+ 4.44
100.0	0.60	0.68	66.67	117.44	+ 76.15

(1) Cross-over occurs at a waste age at emplacement of 35.0 years (between 35-68 yrs: ΔM/M<5%). The 100% increase in repository mass loading is attained for waste ages greater than 86.0 yrs.

(2) Cross-over occurs at a waste age at emplacement of 49.0 years (between 49-82 yrs: ΔM/M<5%).